The Impact of Hurricanes on Cloud-Radiative Forcing over Tropical Oceans

A Thesis Presented

by

Yue Li

to

The Graduate School

in Partial Fulfillment of the

Requirements

for the Degree of

Master of Science

in

Marine and Atmospheric Science

Stony Brook University

August 2007

Stony Brook University

The Graduate School

Yue Li

We, the thesis committee for the above candidate for the
Master of Science degree,
hereby recommend acceptance of this thesis.

Dr. Minghua Zhang (Thesis Advisor)
Professor and Director
Institute for Terrestrial and Planetary Atmospheres
School of Marine and Atmospheric Sciences

Dr. Sultan Hameed (Reader)
Professor
Institute for Terrestrial and Planetary Atmospheres
School of Marine and Atmospheric Sciences

Dr. Nicole Riemer (Reader)
Assistant Professor
Institute for Terrestrial and Planetary Atmospheres
School of Marine and Atmospheric Sciences

This thesis is accepted by the Graduate School

Lawrence Martin
Dean of the Graduate School

Abstract of the Thesis

The Impact of Hurricanes on Cloud-Radiative Forcing over Tropical Oceans

by

Yue Li

Master of Science

in

Marine and Atmospheric Science

Stony Brook University

2007

This research studies the impact of hurricanes on the energy budget at the Top of the Atmosphere (TOA) over tropical oceans from 1983 to 2004. Cloud-Radiative Forcing (CRF) is used to quantify the impact. It is found that in both selected regions (North Atlantic and Northeast Pacific) the CRFs have a strong relationship with hurricane days: both longwave (LW) CRF and shortwave (SW) CRF increase with hurricane days, implying that both of them contribute a warming effect. High cloud and low cloud amount redistribution are found to be responsible for this relationship.

By investigating the individual hurricanes, we find that when a hurricane occurs, LW CRF is increased, while SW CRF is decreased, due to increase of both high and low clouds. However, the impact of hurricanes is not only spatial but temporal. After hurricane disappears, there is significant SW CRF warming anomaly, which is linked

to the possible suppression of low clouds due to hurricanes' temporal impact. Hurricanes' CRF impact is related to their strength, and the average CRFs due to hurricanes are larger in the Northeast Pacific than in the North Atlantic.

Table of Contents

List of Figures

Acknowledgements

I have spent two years of unforgettable life at Stony Brook University, during which I have learned and improved, experiencing anxiety and excitement, despair and hope.

The completion of this work benefits from a lot of people. First and foremost, I would like to thank my thesis advisor, Dr. Minghua Zhang. Without his continuous support and patient guidance, I would not be able to move forward so smoothly. He has provided me with a lot of opportunities to learn and explore the fields of atmospheric science through work on this very interesting project. I am also grateful to my thesis readers, Dr. Sultan Hameed and Dr. Nicole Riemer for their helpful comments and suggestions. I would also like to extend my warmest gratitude to my friends Yanjuan Guo, Yanluan Lin, Wuyin Lin, Tiehan Zhou, Hua Song, Moguo Sun, and all faculties, staffs and colleagues who have helped me. Most of all, I would like to give my special thanks to my wife Qing, for her unconditional love and support throughout this work.

1. Introduction

Hurricanes are tropical cyclones with maximum sustained winds that exceed 64 knots (74mi/hr), where maximum sustained winds mean the highest 1 minute average winds that are observed at the meteorological height of 10m in an unobstructed exposure. Hurricane is the costliest natural disaster in the United States (Pielke et al. 1998). Due to the huge losses caused by hurricanes in recent years, such as Katrina in 2005, attention has focused on the trend of hurricane numbers and their intensities. There has been no previous study however that examines the net effect of hurricanes on the energy budget of the earth-atmosphere system. Several studies have indicated a trend toward more intense hurricanes with increasing global mean temperatures in recent decades (e.g., Trenberth 2005; Emanuel 2005; Webster et al. 2005; Hoyos et al. 2006). Impact of hurricanes on the cloud forcing may constitute a feedback to the global climate.

Hurricanes winds blow in a counterclockwise direction in the Northern Hemisphere (clockwise in the Southern Hemisphere) around the usually calm, cloudless center called the eye. Surrounding the eye is the eyewall, the region with large bands of clouds and most intense winds. Koteswaram (1967) reported that the low pressure core of mature hurricanes could extend into the lower stratosphere up to about 27km. It is well known that clouds play a significant role in the energy budget of the earth-atmosphere system, and cloud-climate interaction constitutes one of the greatest uncertainties in projecting future climate change by global climate models (e.g., Cess et al. 1990, 1996; Potter et al. 2004). Cloud-radiative forcing (CRF) is defined as the impact of clouds on the input of radiative energy to the earth-atmosphere system at the Top of Atmosphere (TOA) (after Zhang et al. 1996). Clouds exert a both cooling effect by reflecting shortwave (SW) radiation back to space and a warming effect by blocking longwave (LW) radiation emitted by the earth’s surface. Whether a cloud will heat or cool the earth depends on its type, altitude and optical properties. The SW CRF is defined as the full-sky net downward SW radiation minus the clear-sky net downward SW radiation, while LW CRF is defined as the clear-sky outgoing LW radiation minus the full-sky outgoing LW radiation, both at the TOA. Typically LW CRF is positive and SW CRF is negative, and the net CRF is the sum of the two. CRFs are quite variable over different regions; however, overall, averaging the effects of all the clouds globally, cooling dominates (Ramanathan et al., 1989; Harrison et al., 1990), which means a net reduction of global energy budget due to the presence of clouds.

There have been extensive studies on the interaction between clouds and other factors in the climate system. Several studies have shown that CRFs have a strong relationship with El Niño-Southern Oscillation (ENSO) (Zhang et al. 1996; Wang et al. 2003), which is directly linked with sea surface temperature (SST) anomalies in the equatorial eastern Pacific. Zhang et al. (1996) found that there is domain dependence between the relationship of CRFs and SST. They also found that over Atlantic and Indian oceans the magnitudes of both LW and SW CRFs decreased with increased SST associated with the 1987 El Niño event, which was contradictory to the known relationship between CRFs and SST, and they reported that it was due to the reduction of the cloud amount (CA) over these two oceans. Studies by Cess et al. (2001) shown that in 1997/98 El Niño year, the collapse of Walker circulation and enhanced upward motion in eastern Pacific caused the redistribution of cloud altitudes in the western and eastern part of Pacific, which may significantly impact the radiation budget of tropical Pacific.

However, there have been no reported studies on the impact of hurricanes on regional CRFs. Studies on hurricane interaction with ocean surface reported sea surface cooling, which is mainly due to mixing of surface and underlying cold water (e.g., Sutyrin 1980; Bender et al. 1993; Ginis 1995). The indirect effects of hurricanes on clouds, such as due to the cooling of surface water, have not been studied.

The objective of this research is to understand how clouds respond to the dynamic forcing of hurricanes over tropical oceans. This study investigates the impacts of hurricanes on CRFs over North Atlantic and Northeast Pacific, respectively. In Section 2, data used and procedure are described. Section 3 presents the main results of this research. The results on North Atlantic and Northeast Pacific will be presented separately. Summary and discussion are given in the last section.

2. Data and Procedure

a. CRF and CA

The CRF data used in our study are FD flux data at the TOA from International Satellite Cloud Climatology Project (ISCCP). We first used FD-MPF monthly data, and then used FD-TOA 3-hourly data. The data include fluxes under both clear-sky and full-sky conditions. Detailed description of the ISCCP-FD data can be found in Zhang et al. (2004). ISCCP-D2 dataset are used for CA, and the full documentation for the ISCCP-D2 dataset is in Rossow et al. (1996). We used VIS/IR CA data, which means that clouds are detected by infrared radiation test at nighttime and by separate visible and infrared radiation tests in daytime. Both of the data span from July 1983 to December 2004 and have a 2.5° lat × 2.5° long resolution. CRFs in the months when most hurricanes occur are used for North Atlantic (July to November, 10°N-35°N, 20°W-80°W) and Northeast Pacific (June to October, 10°N-35°N, 105°W-150°W). And the same time and spatial range is applied to monthly CA data.

b. Hurricane

The hurricane data are taken from National Hurricane Center / Tropical Prediction Center best track data for North Atlantic and Northeast Pacific hurricanes. More information can be found in Jarvinen et al. (1984) and Davis et al. (1984). We take the data from 1983 to 2004 as consistent with CRF and CA data. This hurricane dataset contains 6-hourly hurricane center locations which we later use to trace CRFs around hurricane centers.

Fig. 1 shows the time variation of hurricane days over North Atlantic and over Northeast Pacific. Hurricane days refer to all the days when a hurricane is detectable in a year. If more than one hurricane were present on the same day at one basin, it was counted as only one hurricane day. There are strong interannual variations in hurricane days in both basins. On average, there are more high hurricane days in the Northeast Pacific than in the North Atlantic.

c. SST

To find out the effect of ENSO on CRFs and the impact on this study, Hadley center December, January and February (DJF) SST anomalies of Niño 3.4 region (120°W-170°W, 5°S- 5°N) from 1983 to 2004 are used as ENSO index (Fig. 2). This index is assigned to the year from which January and February SSTs are taken. It is seen that El Niño years are associated with high positive anomalies of the index (e.g., 1982-1983, 1991-1992, 1997-1998), while high negative anomalies represent La Niña years (e.g., 1988-1989, 1998-1999).

For each basin, regional and seasonal averaged CRFs are regressed against ENSO index and the residuals are taken as the ENSO filtered CRFs. Fig. 3 compares the original CRFs and the ENSO filtered CRFs over North Atlantic. It can be observed that ENSO signal in CRFs is not large since the ENSO filtered CRFs are very similar to the original. This may be due to that CRFs used here are primarily from summer months and regionally averaged, while ENSO is strongest in winter. The comparison for Northeast Pacific is shown in Fig. 4. As anticipated ENSO has a larger impact on Northeast Pacific CRFs, especially over LW CRFs, which is consistent with the finding of Zhang et al. (1996). However, this impact is still negligible in our study. Hence, in the following parts, only the original CRFs are used.

3. Results

a. North Atlantic

Fig. 5a) shows that the averaged LW CRF increases with hurricane days. Thus, when there are more hurricane days, there is more cloud trapping of LW radiation, which means a warming effect. The relationship between SW CRF and hurricane days in Fig. 5b) also shows an increase trend. Note that SW CRF is negative, thus, there is less SW radiation reflected back to space with more hurricane days, which is also a warming effect. Errors in S represent 95% confidence level of the regression slopes, where Student's t test is used (the same below).

It is known that low clouds have a large impact on SW radiation due to their high albedo and thus cool the earth's surface, while high and thin clouds primarily transmit SW radiation and at the same time trap LW radiation from the earth, and overall a warming effect. So we examined the relationship between hurricane days and both high and low clouds. Fig. 6 indicates that with increasing hurricane days, high clouds become larger and low clouds get less. So from Figs. 5 and 6, the conclusion is drawn that with more hurricanes days, high clouds are increased bringing in more LW warming, while low clouds are decreased which results in SW warming because the cooling effect is suppressed.

To better highlight this point, composite studies were conducted to see the spatial radiative effect of hurricanes. Five years with highest and lowest hurricane days are chosen, and the spatial CRFs are averaged for each 2.5° × 2.5° grid for these two 5- year, respectively. Figs. 7a) and b) give LW CRFs of the highest and lowest

5-year composite, and the difference of the two is given is c), which shows the change of LW CRF due to increase in hurricanes days, if ideally other conditions are constant. It can be observed that LW CRF increases from Eastern Atlantic towards Western Atlantic. Fig. 7c) indicates that warming due to more hurricane days occurs in most regions, strongest in Caribbean Sea, which is the typical hurricane active region. The second peak is located east of Puerto Rico, while cooling effect is evident north of Cuba. Unlike the distribution of LW CRF, SW CRF in Figs. 8a) and b) is weakest in central Atlantic. The change of SW CRF between the two composites is shown in Fig. 8c). In the western part of the domain, it is opposite to LW in sign, indicating a SW cooling. Over the many parts of the region, however, it is positive. Its regional average is about 2.19 W/m^2. The net CRF 5-year difference in Fig. 9c) is almost uniformly positive, a combining warming effect due to both LW and SW CRFs.

The same composite studies were carried out on high clouds (Fig. 10) and low clouds (Fig. 11). It is seen from Fig. 10 that the distribution of high CA matches that of LW CRF quite well. Fig. 10c) shows that in Caribbean Sea, high clouds increase as large as 8%, which results in the largest LW CRF warming. It is also observed that not only the sign but the magnitudes in Figs. 7c) and 10c) are very close. The distribution of low CA (Figs. 11) shows a dissimilar pattern with SW CRF, with highest low CA at Eastern Atlantic and lowest value at Caribbean Sea. The SW CRF in the Eastern Atlantic is from the low clouds, while that over the Caribbean Sea is due to deep clouds. Uniformly decrease of low CA is shown in Fig. 11c). Because low clouds may be shielded from high clouds in the ISCCP data, reduction of low clouds may be related with increase of high clouds. We can rule out this possibility because the magnitude of the reduction in low clouds in the Eastern Atlantic is larger than that of the increase in high clouds, where the SW CRF warming is the largest. After regional average, the changes of LW, SW and high CA are all positive, and low CA decrease is almost everywhere, consistent with our previous findings.

To understand whether the change of the seasonally averaged CRF is due to the direct impact of hurricanes or other indirect effects, we carried out composite study as follows: for all available hurricane center locations (6 hourly), the instantaneous LW CRFs at the center and surrounding areas are averaged to get a single result. Due to the reason that SW CRF highly depends on time and location, which is fundamentally the incoming solar radiation, SW CRF is normalized by first divided by instantaneous incoming solar radiation **I** and then averaged, and then multiplied by regional mean of hurricane season incoming solar radiation. Another factor is solar zenith angle. Because when solar zenith angle is large, solar insolation decreases significantly, which will introduce large errors, so only values of $\mathbf{I} \geq 100\ \mathrm{W/m^2}$ are included in the calculation.

$$\overline{SW} = \left(\sum_{I \geq 100} \frac{SW}{I} \Big/ n \right) * I_{seasonal\_mean} \qquad (1)$$

where $\overline{SW}$ is the normalized SW CRF, SW is the original instantaneous SW CRF, n is the total number when $\mathbf{I} \geq 100\ \mathrm{W/m^2}$, and $I_{seasonal\_mean}$ is the regional mean of hurricane season incoming solar radiation.

Fig. 12 gives the results for LW, SW and Net CRFs. The latitude and longitude of the hurricane center in the figure is the average of all hurricane center locations. It shows that LW CRF has a strong warming effect with maximum 90 W/m^2 in the center, which is about 65 W/m^2 more than the North Atlantic mean. It is also noticeable that individual hurricanes can influence the surrounding area CRFs as large as 5 degrees, which is about 500 km. One interesting observation from Fig. 12a) is that the regions of CRFs impacted by hurricanes extend shortest to the west of the hurricane center, which may be due to the interaction with lands. Fig. 12b) shows that hurricanes have a strong cooling effect as large as –140 W/m^2, compared to the estimated regional monthly mean –40 W/m^2, which indicates that when hurricane passages, it causes intense SW CRF cooling. However, since Fig. 5b) shows a SW warming effect, and there is overall SW warming and low CA decrease (Figs. 8c) and 11c)), so we propose that the SW CRF cooling due to hurricane passage is instantaneous, while the temporal radiative effect of hurricanes suppresses low CA formation inducing SW warming effect, which predominates in the seasonal average.

To amplify this point, composite study was conducted as Figs. 7-9, but using data excluding the time when there was a detectable hurricane in the basin (Figs. 13 -15). It should be noted that when we were doing this, we excluded hurricane occurrence time from the months in the seasonal statistical study (July – November for North Atlantic and June – October for Northeast Pacific). This is important for Northeast Pacific because there are more hurricanes days out of the selected months in that basin. The highest hurricane days are 99 and 112, and the mean hurricane days are 52 and 68 for North Atlantic and Northeast Pacific, respectively. While the total days for each hurricane season taken here is only 153, even taking into account that some hurricane days are not in the selected months, it is hardly possible that the large scale atmospheric motion induced by hurricanes does not impact the other days. The spatial patterns in Figs. 13-15 are similar to Figs. 7-9. It is noted in Fig. 13c) that the magnitudes of positive values are smaller while that of negative values are larger, compared with Fig. 7c), implying an instantaneous LW warming effect due to hurricanes. And it is opposite in Fig. 14c) which can be compared with Fig. 8c), confirming that hurricane passage causes a SW cooling effect, consistent with Fig. 12b). Noted that the regional average of Fig. 14c) is 3.44 W/m^2 while that of Fig. 8c) is only 2.19 W/m^2, so it shows a strong SW warming effect due to hurricanes' temporal radiative effect. The above discussion implies that the occurrence of hurricanes results in instantaneous increase of both high and low clouds, causing both LW warming and SW cooling, however, after hurricane disappears, it is associated with sharp decrease of low clouds, bringing in SW warming effect, and the overall seasonal average effect of both LW and SW CRFs are warming.

b. Northeast Pacific

The relationship between hurricane days and CRFs over Northeast Pacific shown in Fig. 16 is consistent with that of North Atlantic. It is noticeable that though the magnitude of LW CRF of Northeast Pacific is comparable with that of North Atlantic, the SW CRF is much less (stronger), implying more low CA in this region. Fig. 17 shows that it is the same relationship between high and low CA and hurricane days, indicating the effects of hurricanes are similar in both regions.

Figs. 18 a) and b) show the comparison of LW CRFs for the two composites of high and low hurricane days. The spatial pattern of LW CRF indicates a more latitudinal distribution close to equator compared with North Atlantic, and even though the regional mean is about the same, the longitudinal change of magnitude is much larger in this region. The largest warming effect in Fig. 18c) is west of Mexico, which is also a hurricane active region. Figs. 19a) and b) show that SW CRFs strongest cooling is in the central area of Eastern Pacific, as strong as – 90 W/m^2. Fig. 19c) indicates that the largest SW cooling due to hurricane day difference is close to the positive peak in Fig. 18c) in location, and it has a high positive peak north of it. The pattern of net CRF follows that of SW CRF due to its much larger magnitude (Fig. 20). It is noted that the net warming anomaly is as large as 20 W/m^2 in Fig. 20c), which is a remarkable amount if totally due to hurricane day difference. And the regional average is also higher than that of North Atlantic, which is related to the average hurricane category.

The pattern of high clouds corresponds well with LW CRF, increasing in amount from North towards equator, indicating this pattern is primarily determined by the temperature distribution (Fig. 21). The most pronounced difference compared with North Atlantic is that the spatial pattern of low clouds is consistent with that of SW CRF generally, and also there is low CA decrease in most regions (Fig. 22).

The composite study of individual hurricanes as did in Fig. 12 is given in Fig. 23. The CRFs impact is more symmetric, compared to Fig. 12. The center peak LW and SW CRFs are 100 W/m^2 and –170 W/m^2, respectively, both are stronger than that of North Atlantic, because of more high category hurricanes in this region. It should be pointed out that the averaged latitude of all available hurricane locations in the Northeast Pacific is about 17°N, which is about 10° less than that of North Atlantic hurricanes. This indicates that North Atlantic hurricanes can impact CRFs of higher latitudes, and though low latitude Caribbean Sea is the hurricane active region, hurricanes often move northward, which brings great possibility to hit land, while in contrast, hurricanes in the Northeast Pacific usually head in a zonal direction.

The same procedure is taken to exclude the hurricane occurrence time over Northeast Pacific (Figs. 24-26). By comparing Figs. 18a) and b) and Figs. 24a) and b), it is noticed that LW CRF is more zonal in Fig. 24, and the same condition on SW CRF, implying the strong instantaneous effect due to hurricanes. The same conclusion can be drawn as from Figs. 13-15.

Finally, we examined the relationship between hurricane days and total clouds. There is no statistical relationship found (Fig. 27). This indicates that total CA does not simply increase with hurricane days, but high and low CA have their specific relationship with hurricane days and are redistributed.

4. Conclusion and Discussion

We have reported that when hurricanes occur, they result in both LW CRF warming and SW CRF cooling effect, which is considered due to increase of both high and low clouds. However, the temporal and spatial effects of hurricane occurrences are associated with suppression of low clouds which overwhelms the increase of low clouds during hurricane time. So overall, high clouds are increased while low clouds are decreased in a more active hurricane season, both contributing to warming CRF effect.

Considering the internal structure of hurricanes, we propose to explain it as follows: strong convergence in the hurricanes at the low level and intense updraft in the eyewall and rainbands transport massive amount of moisture to high level which facilitate the formation of high clouds, while divergence and downward motion at the outward bound in the high level suppress the low clouds. Jorgensen et al. (1985) reported that in both eyewall and rainband regions updrafts dominated over downdrafts, in both mass transport and number. When there are more hurricane days, which indicates hurricane’s impact is greater, more high clouds are formed while more low clouds are suppressed. However, it should be noted that the suppression of low clouds is not necessarily an instantaneous but could be a temporal effect. No previous studies have examined whether low clouds significantly decrease before or after hurricane passage. This assumption needs to be examined, such as using a high resolution hurricane model. Our study has demonstrated the association of hurricanes with suppressed low clouds and more abundant high clouds when averaged for a whole season.

There are uncertainties in this study. The first is the selection of the region, especially for the seasonally mean study. Ideally the region should be large enough to include the tropical ocean region which covers most hurricane locations but not too large since this study is to focus on tropical oceans. However, hurricanes frequently head northward and become extratropical storms, particularly in the North Atlantic. We extend the north boundary only to 35°N as a compromise. We did try to change the region size, but only latitudinally, and no statistical difference from the current results is found. The second uncertainty is the hurricane index. The one used here is hurricane days, better than hurricane number, but it can be improved, such as using hurricane Power Dissipation Index (Emanuel, 1998) or Accumulated Cyclone Energy (Camargo et al., 2005). And here all hurricane days are counted for each year while the hurricane months are fixed, which also brings errors, since some hurricane days are not in those months, especially in the Northeast Pacific. The third is that we only include hurricane days but not tropical storms. However, in this study we count hurricane days for each detectable day, while at the developing and dissipation stages the strength of the hurricane can be less than mature tropical storms. So it is also advised to include all tropical storms or define a strength threshold. The fourth is that the period we choose is relatively short, constrained by the data availability. It is known that hurricane has decadal to multi-decadal variability, which may bring us with false conclusions.

We propose several ways to confirm the results of this study: 1. to examine the

CA change using daily cloud data; 2. to use a more appropriate hurricane index and use longer time and more precise data, if available; 3. to study more regions, i.e., Northwest Pacific, North Indian Ocean, Southern Hemisphere Ocean; 4. to simulate the CRF and CA change due to hurricane occurrence with a high-resolution hurricane model, which is the ideal way if the model includes correct microphysical, dynamical processes and has enough resolution.

References:

Bender, M. A., I. Ginis, and Y. Kurihara, 1993: Numerical simulations of tropical cyclone-ocean interaction with a high-resolution coupled model. J. Geophys. Res., 98, 23245-23262.

Camargo, S. J., Sobel, A. H., 2005: Western North Pacific tropical cyclone intensity and ENSO. J. Climate, 18, 2996-3006.

Cess, R. D., and Coauthors, 1990: Intercomparison and interpretation of climate feedback processes in 19 atmospheric general circulation models. J. Geophys. Res., 95, 16601-16615.

Cess, R. D., and Coauthors, 1996: Cloud feedback in atmospheric general circulation models: An update. J. Geophys. Res., 101, 12791-12794.

Cess, R. D., M. H. Zhang, P. H. Wang, B. W. Wielicki, 2001: Cloud structure anomalies over the tropical Pacific during the 1997/98 El Niño, Geophy. Research Letters, 28, 4547-4550.

Davis, M. A. S., G. M. Brown, P. Leftwish, 1984: A Tropical Cyclone Data Tape for the Eastern and Central North Pacific Basins, 1949-1983: Contents, Limitations, and Uses. NOAA Technical Memorandum NWS NHC 25.

Emanuel, K. A., 1998: The power of a hurricane: An example of reckless driving on the information superhighway. Weather 54, 107-108.

Emanuel, K. A., 2005: Increasing destructiveness of tropical cyclones over the past 30 years. Nature, 436, 686-688.

Ginis, I., 1995: Ocean response to tropical cyclones. Global Perspectives on Tropical

Cyclones, R. Elsberry, Ed., World Meteorological Organization, 198-260.

Harrison, E. F., Minnis, P., Barkstrom, B. R., Ramanathan, V., Cess, R. D., Gibson, G. G., 1990: Seasonal variation of cloud radiative forcing derived from the Earth radiation budget experiment. J. Geophys. Res., 95, 18687-18703.

Hoyos, C.D., P.A. Agudelo, P.J. Webster, and J.A. Curry, 2006: Deconvolution of the factors contributing to the increase in global hurricane intensity, Science, 312 (5770), 94-97.

Jarvinen, B. R., Neumann, C. J., Davis, M. A. S., 1984: A Tropical Cyclone Data Tape for the North Atlantic Basin, 1886-1983: Contents, Limitations, and Uses. NOAA Technical Memorandum NWS NHC 22.

Jorgensen, D. P., E. J. Zipser, M. A. LeMone, 1985: Vertical Motions in intense hurricanes. J. Atmos. Sci., 42, 839-856.

Koteswaram, P., 1967: On the structure of hurricanes in the upper troposphere and lower stratosphere. Mon. Wea. Rev., 95, 541-564.

Pielke R. A., Landsea, C. W., 1998: Normalized Hurricane Damages in the United States: 1925-95. Wea. Forecasting, 13, 621-631.

Potter G., Cess. R. D., 2004: Testing the impact of clouds on the radiation budgets of 19 atmospheric general circulation models, J. Geophys. Res., 109, D02106, doi:10.1029/2003JD004018.

Ramanathan, V., R. D. Cess, E. F. Harrison, P. Minnis, B. R. Barkstrom, E. Ahmad, and D. Hartmann, 1989: Cloud-Radiative Forcing and Climate: Results from the Earth Radiation Budget Experiment. Science, 243, 57-63.

Rossow, W. B., A. W. Walker, D. E. Beuschel, M. D. Roiter, 1996: International Satellite Cloud Climatology Project (ISCCP) Documentation of New Cloud Dataset. WMO/TD-No. 737, World Meteorology Organization, 115pp.

Sutyrin, G. G., 1980: Response of the upper layer of the ocean to a moving typhoon. Meteor. Hydrol., 9, 48-55.

Wang, P. H., Minnis, P., Wielicki, B. A., Wong, T., Cess, R. D., Zhang, MH, Vann, L. B., Kent, G. S., 2003: Characteristics of the 1997/1998 El Niño cloud distribution from SAGE II observations, J. Geophys. Res., 108(D1), 4009, doi:10.1029/2002JD002501.

Webster, P. J., Holland, G. J., Curry, J. A., Chang, H. R., 2005: Changes in tropical cyclone number, duration, and intensity in a warming environment. Science, 309, 1844-1846.

Trenberth, K., 2005: Uncertainty in hurricanes and global warming. Science, 308, 1753-1754.

Zhang, MH, Cess, R. D., Xie, SC, 1996: Relationship between cloud radiative forcing and sea surface temperatures over the entire tropical oceans. J. Climate, 9, 1374-1384.

Zhang, Y., W. B. Rossow, A. A. Lacis, V. Oinas, and M. I. Mishchenko, 2004: Calculation of radiative fluxes from the surface to top of atmosphere based on ISCCP and other global data sets: Refinements of the radiative transfer model and the input data, J. Geophys. Res., 109, D19105, doi: 10.1029/2003JD004457.

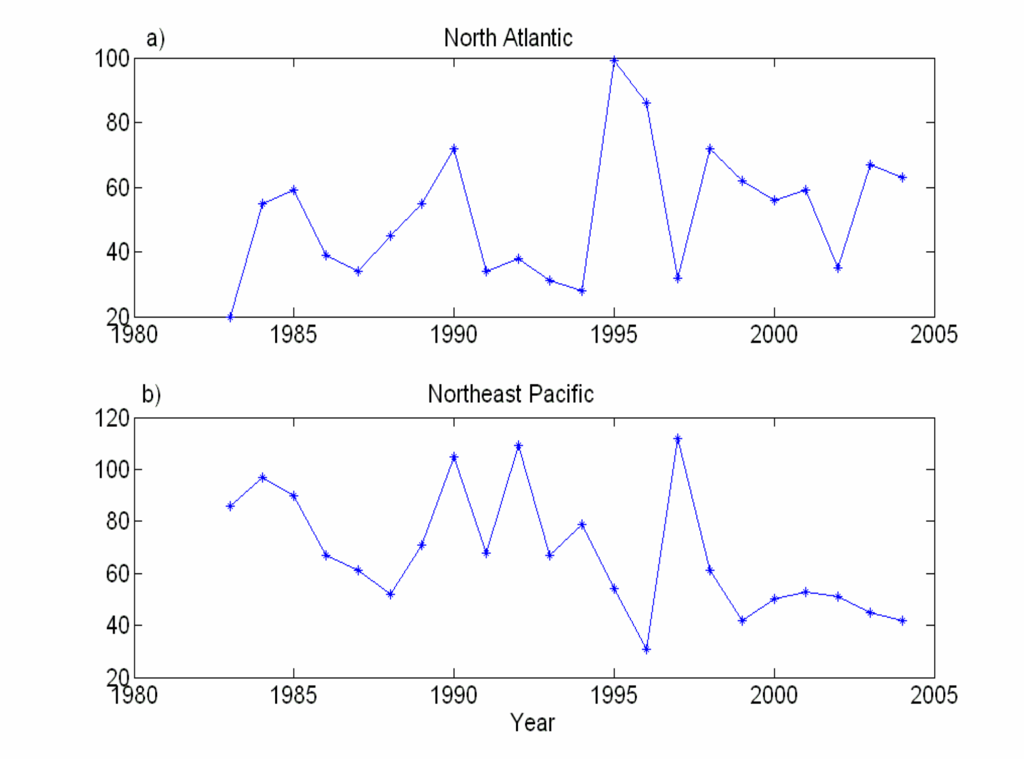

Fig. 1. Time Variation of hurricane days for a) North Atlantic b) Northeast Pacific. Hurricane days refer to all the days when a hurricane is detectable. Only one day is counted for each basin if more than one hurricane occurred on the same day for each basin.

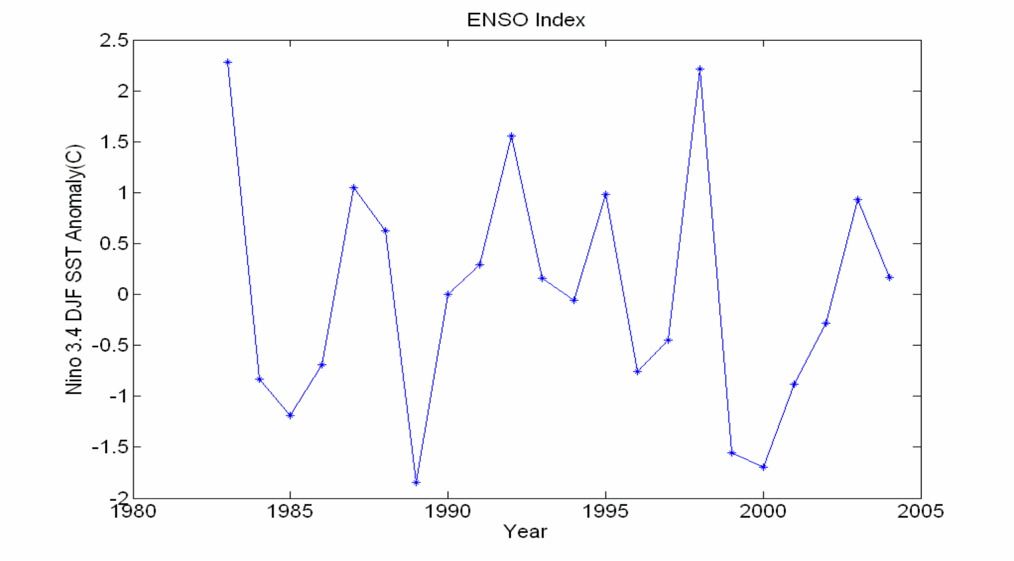

Fig. 2. Time variation of ENSO Index. Hadley center DJF SST for Niño 3.4 region is used, and SST anomalies are obtained by removing the mean of this period to be used as ENSO index.

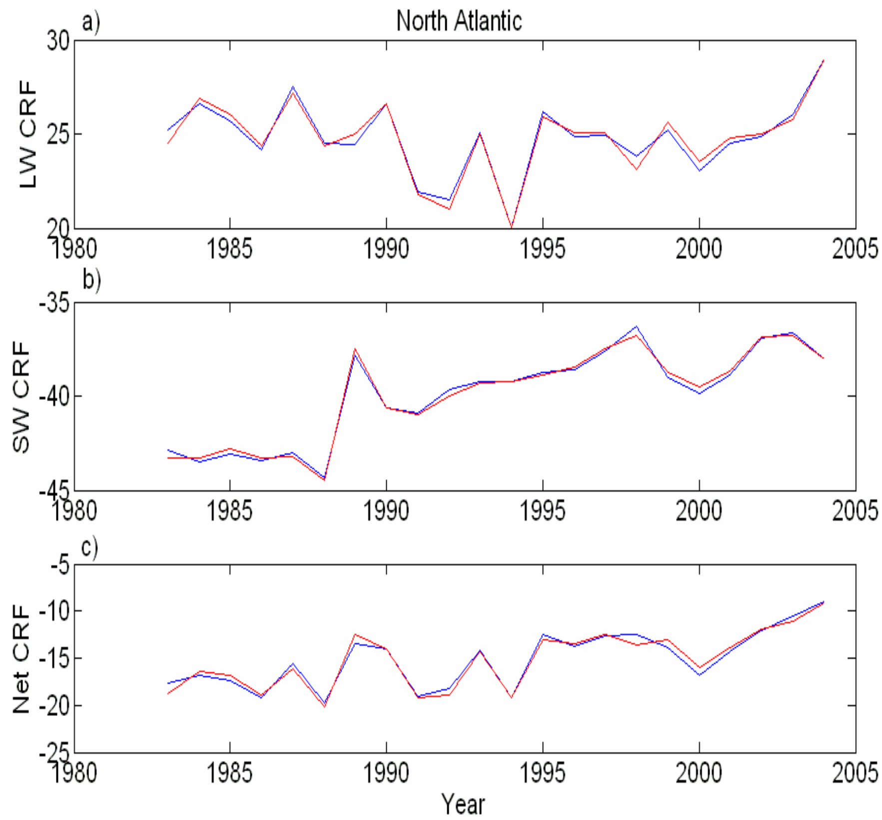

Fig. 3. Comparison of Original CRFs and ENSO filtered CRFs for North Atlantic basin (in W/m^2). The red line is the original CRFs, and the blue line is the ENSO filtered CRFs for a) LW b) SW c) Net.

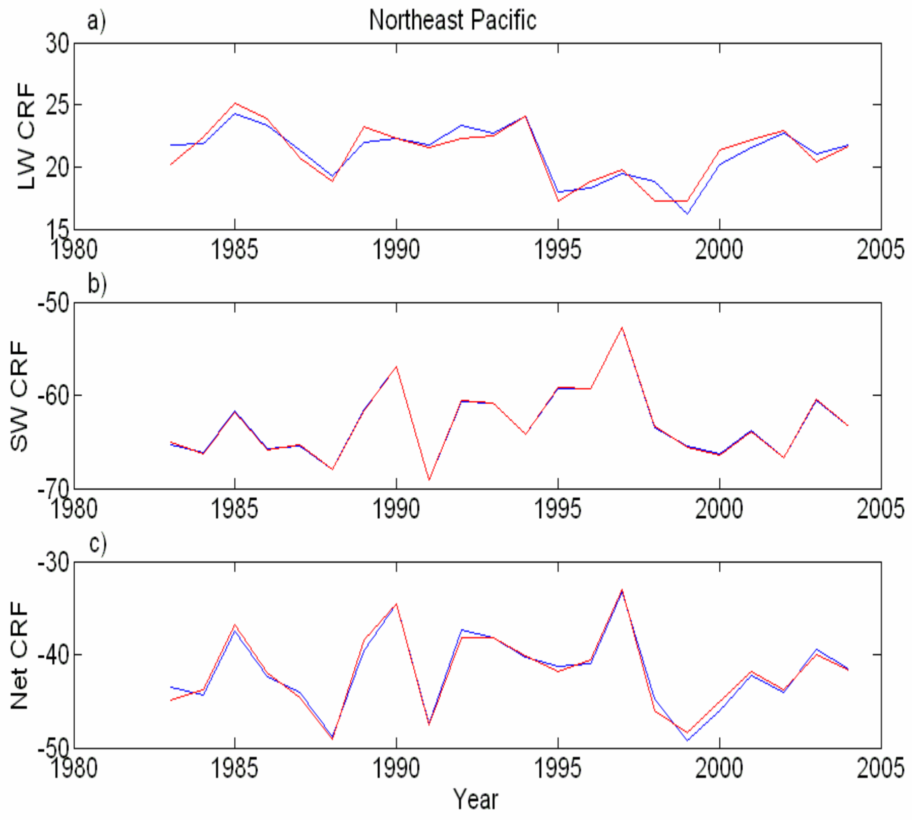

Fig. 4. Comparison of Original CRFs and ENSO filtered CRFs for Northeast Pacific basin (in W/m^2). The red line is the original CRFs, and the blue line is the ENSO filtered CRFs for a) LW b) SW c) Net.

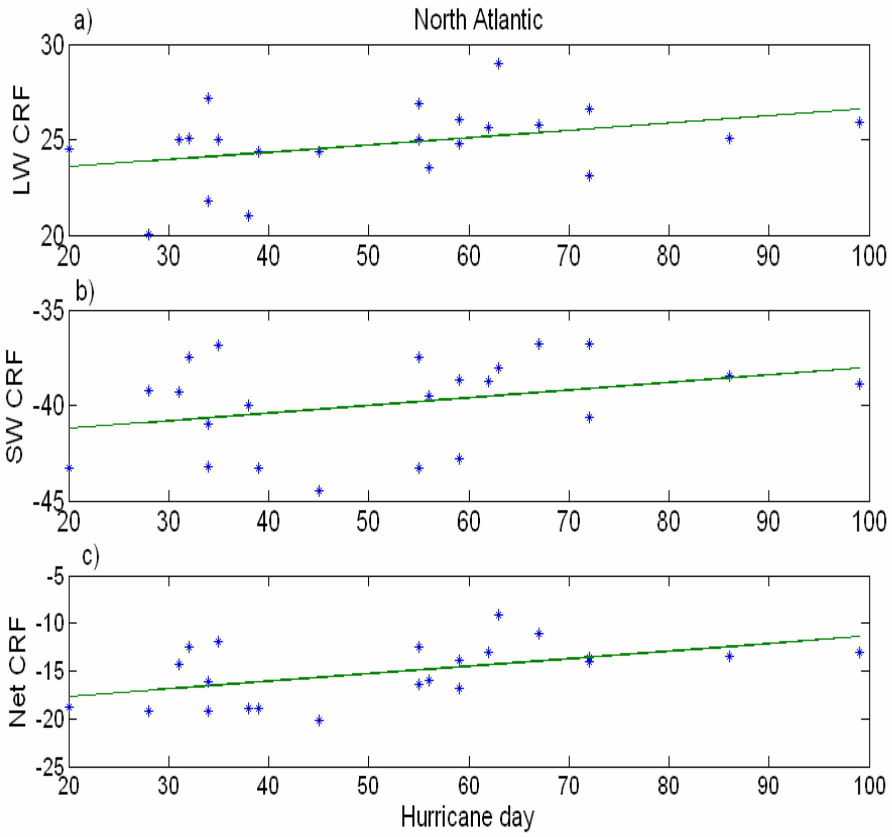

Fig. 5. Relationship of CRFs (in W/m^2) and hurricanes days for North Atlantic.

a) LW, S = 0.04 ± 0.04, R = 0.38

b) SW, S = 0.04 ± 0.05, R = 0.33

c) Net, S = 0.08 ± 0.06, R = 0.51

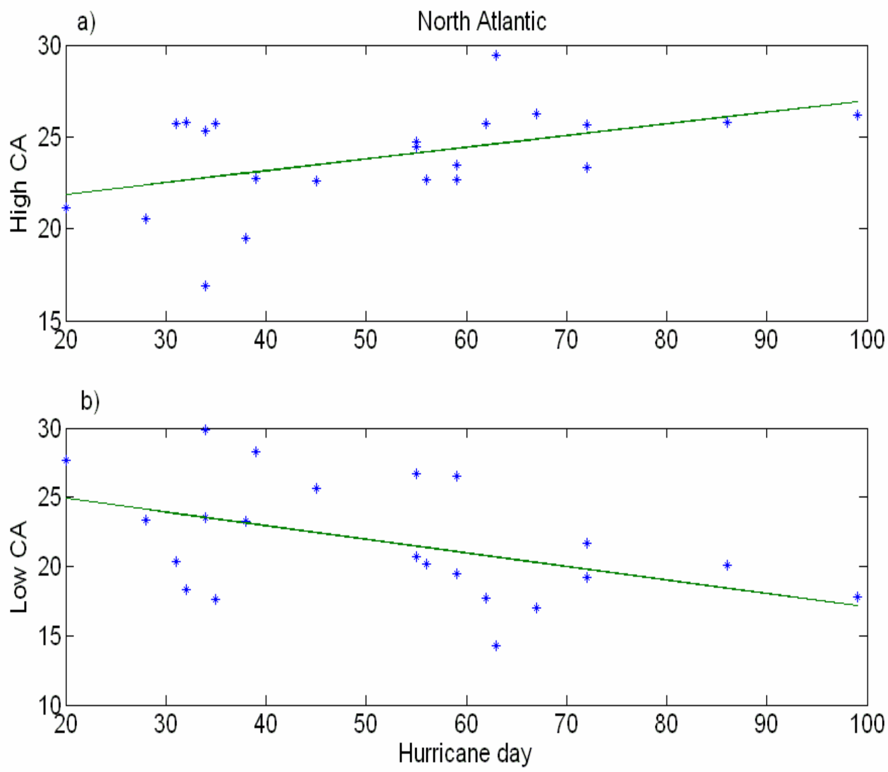

Fig. 6. Relationship of CA (in %) and hurricane days for North Atlantic.
a) High CA, S = 0.06 ± 0.05, R = 0.47
b) Low CA, S = –0.10 ± 0.09, R = –0.47

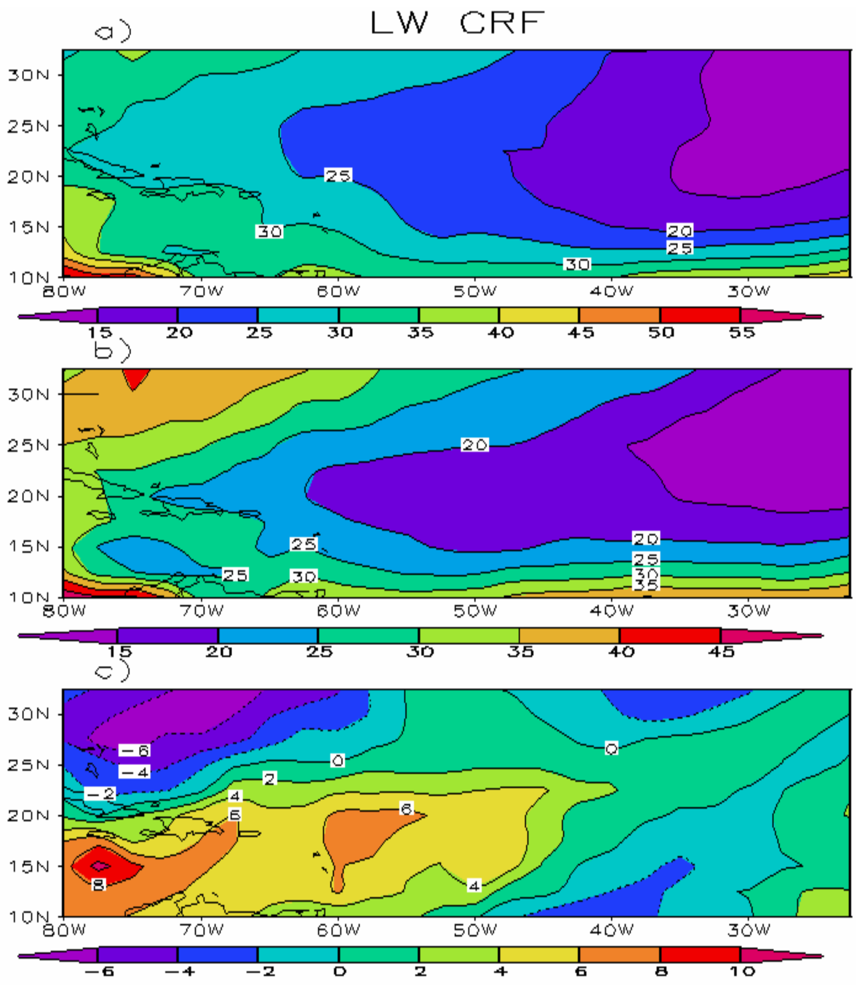

Fig. 7. Composite study of North Atlantic LW CRF (in W/m^2). a) 5-year average of highest hurricane days. b) 5-year average of lowest hurricane days. c) the difference between a) and b).

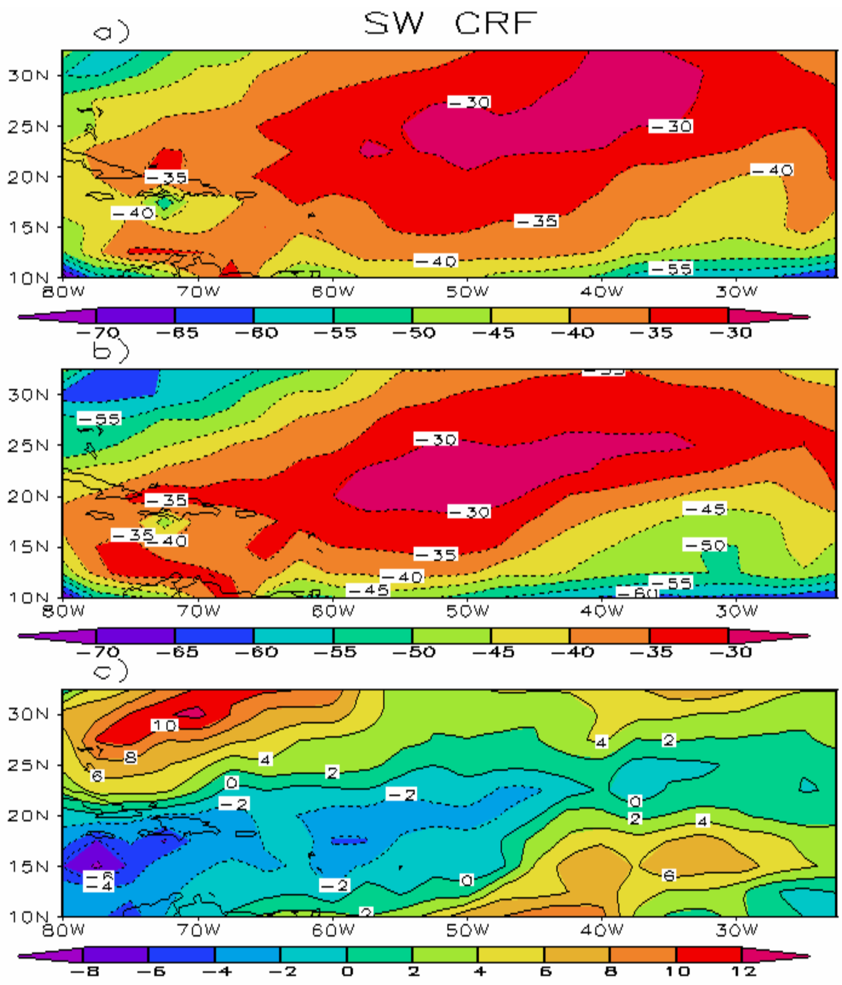

Fig. 8. Composite study of North Atlantic SW CRF (in W/ m^2). a) 5-year average of highest hurricane days. b) 5-year average of lowest hurricane days. c) the difference between a) and b).

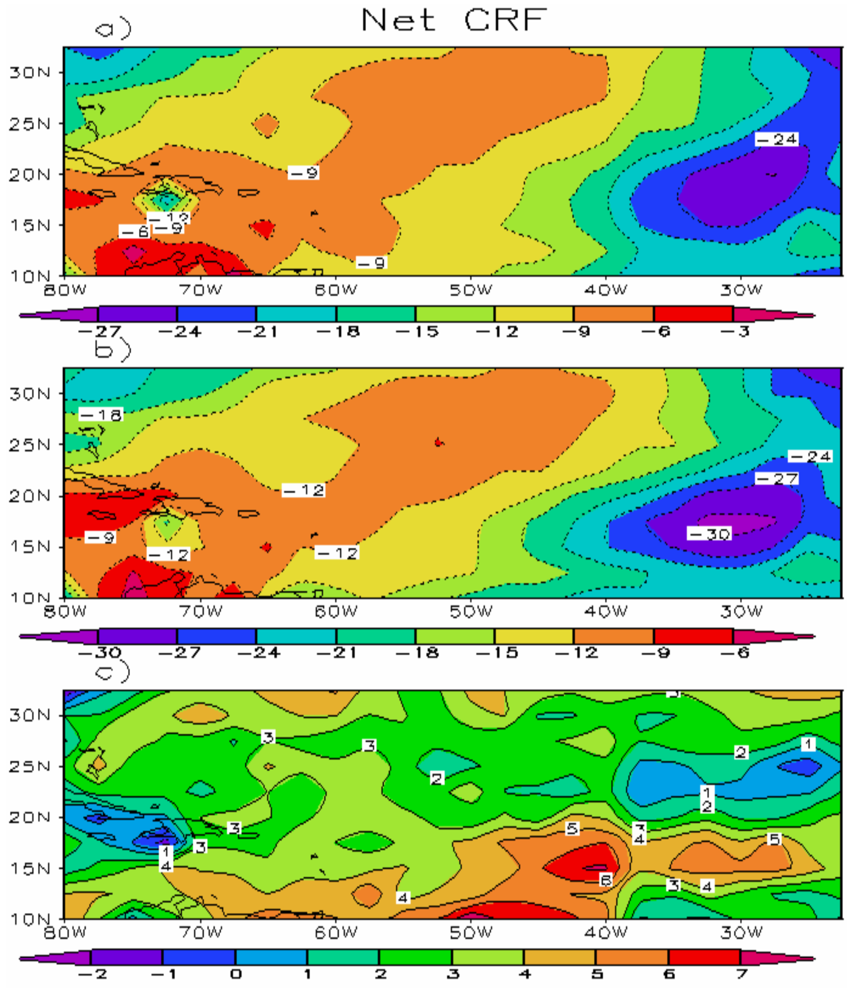

Fig. 9. Composite study of North Atlantic Net CRF (in W/m^2). a) 5-year average of highest hurricane days. b) 5-year average of lowest hurricane days. c) the difference between a) and b).

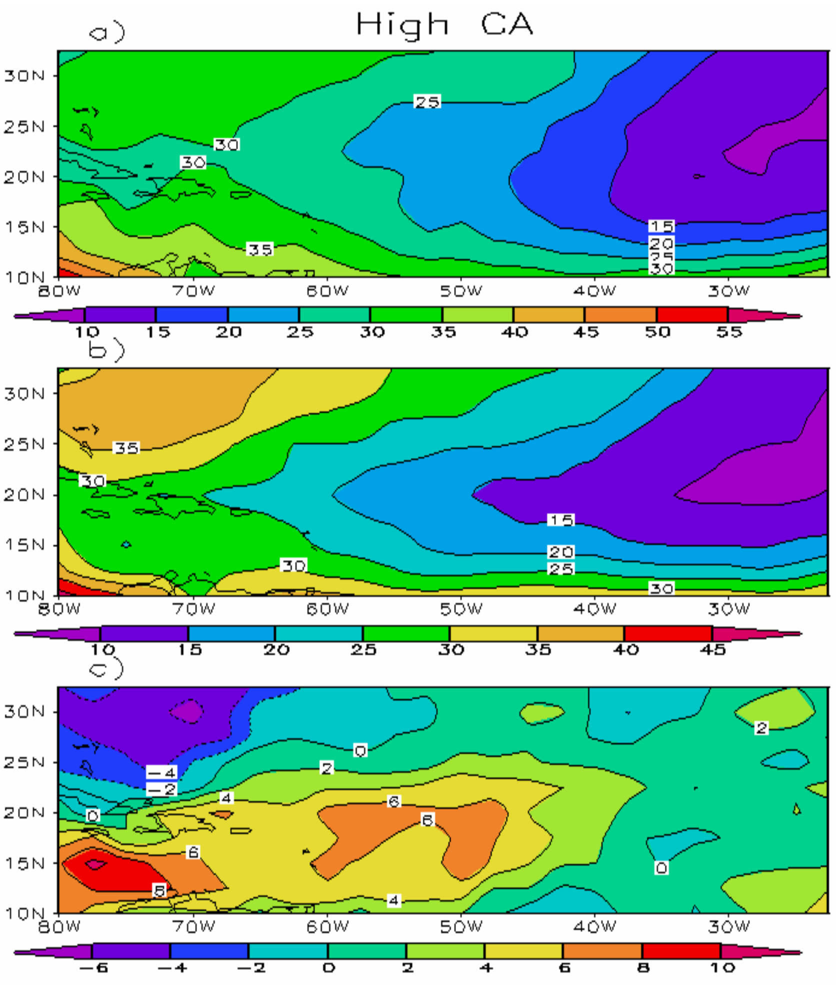

Fig. 10. Composite study of North Atlantic High CA (in %). a) 5-year average of highest hurricane days. b) 5-year average of lowest hurricane days. c) the difference between a) and b).

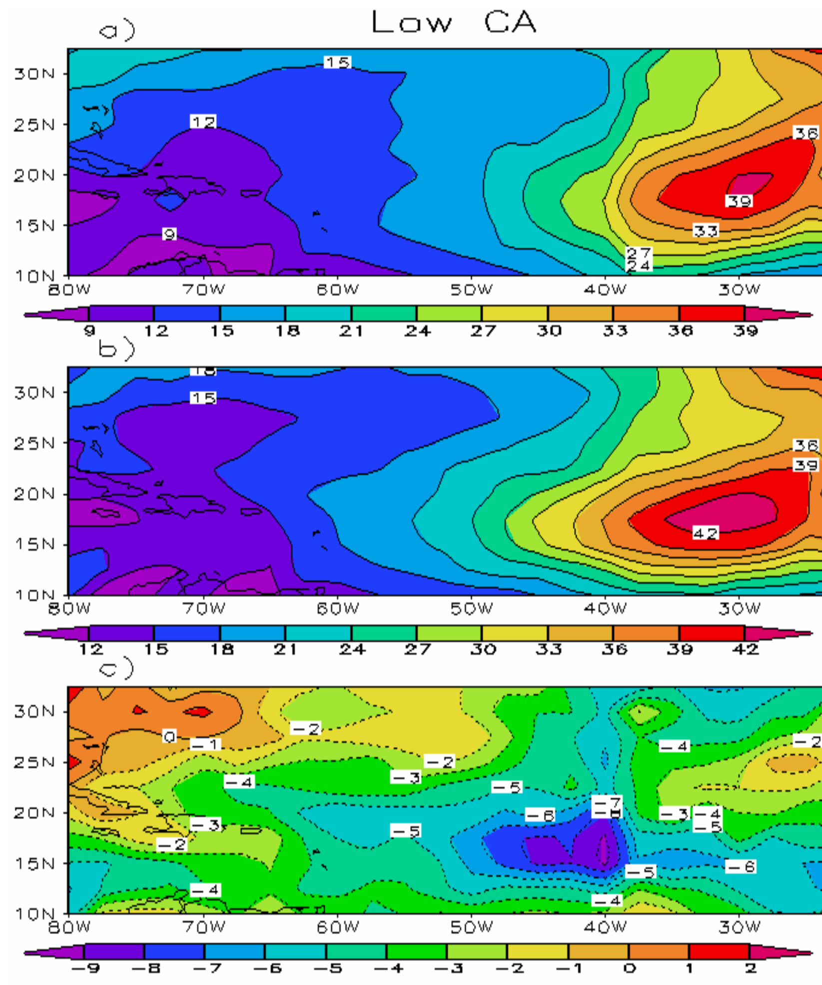

Fig. 11. Composite study of North Atlantic Low CA (in %). a) 5-year average of highest hurricane days. b) 5-year average of lowest hurricane days. c) the difference between a) and b).

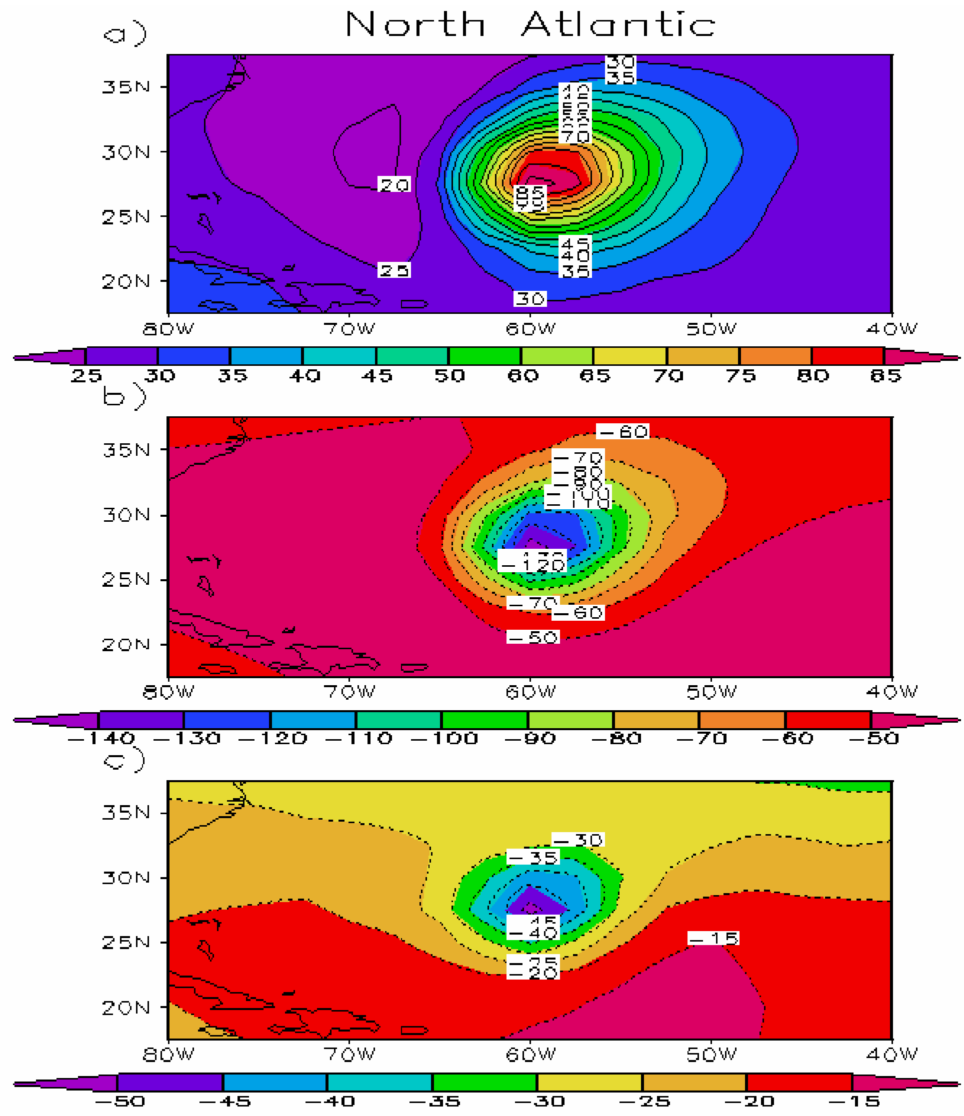

Fig. 12. Composite study of North Atlantic individual hurricanes CRFs (in W/m^2). All detectable hurricane center locations from 1983-2004, which are available every 6 hours, are taken as the center of a moving coordinate, and instantaneous CRFs are averaged relative to the coordinate center. Latitudinally 20 degrees on each side of hurricane center, and longitudinally 10 degrees on each side. The lat/long of hurricane center in the graph is the average of all available hurricane location for North Atlantic. a) LW b) SW c) Net.

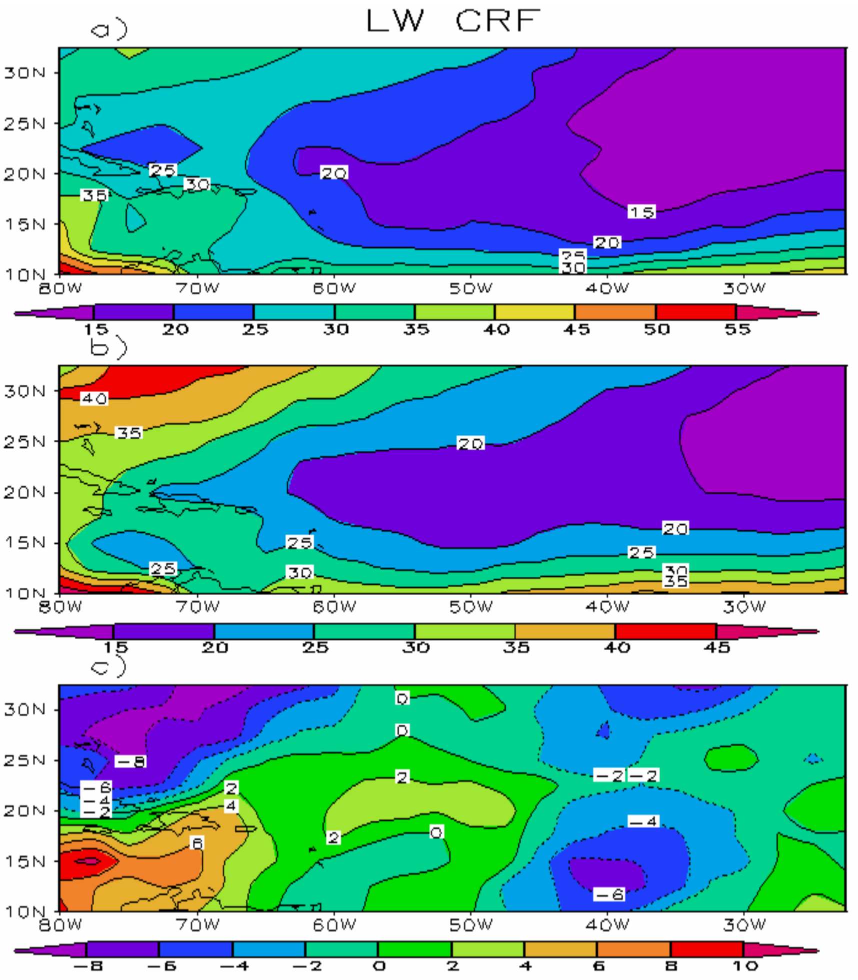

Fig. 13. Composite study of North Atlantic LW CRF (in W/m^2). a) 5-year average of highest hurricane days but excluding all the time having detectable hurricanes b) 5 year average of lowest hurricane days but excluding all the time having detectable hurricanes c) the difference between a) and b).

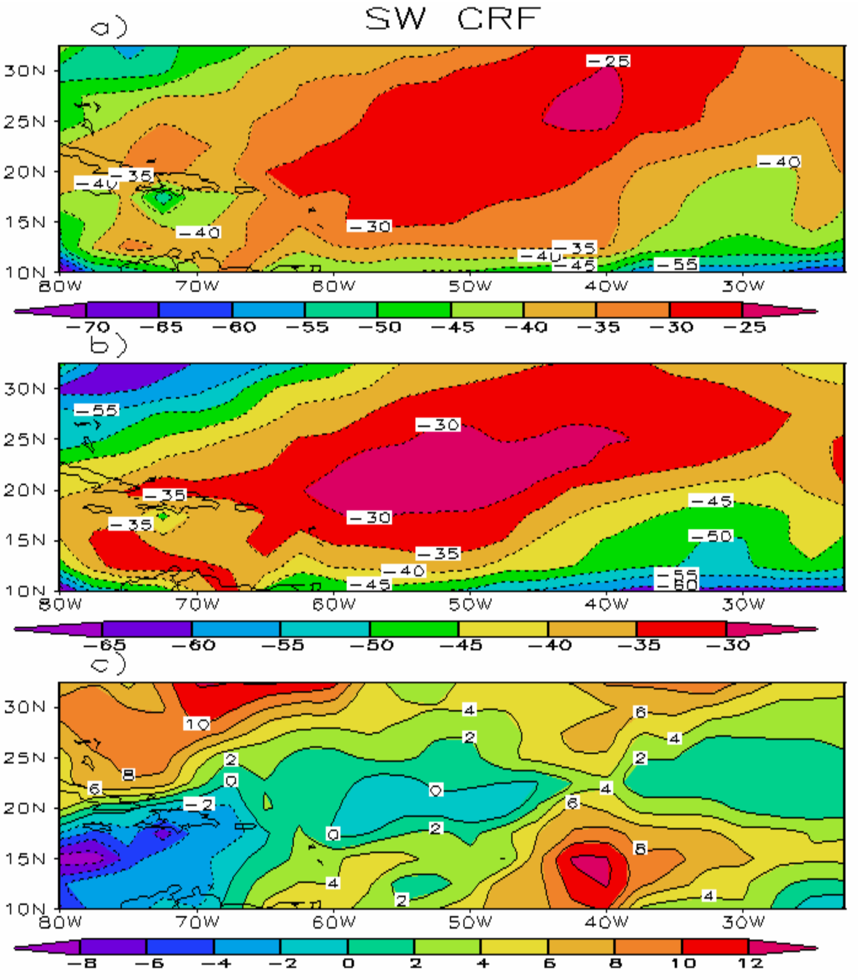

Fig. 14. Composite study of North Atlantic SW CRF (in W/ m^2). a) 5-year average of highest hurricane days but excluding all the time having detectable hurricanes b) 5 year average of lowest hurricane days but excluding all the time having detectable hurricanes c) the difference between a) and b).

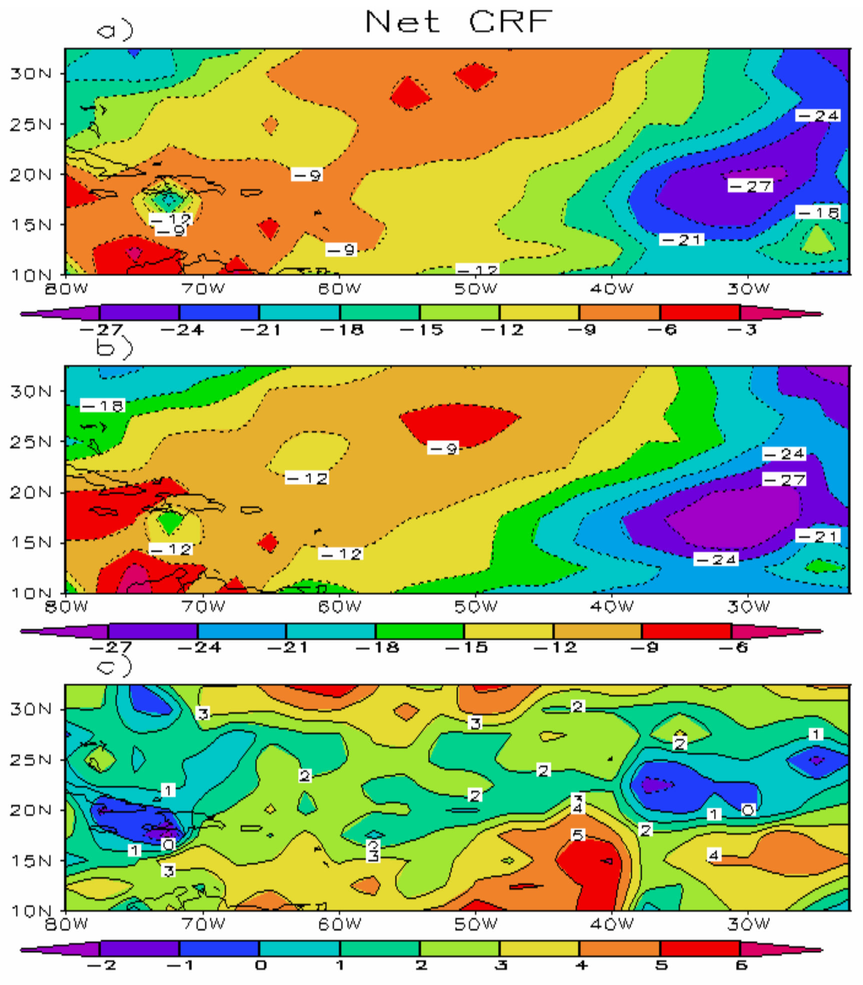

Fig. 15. Composite study of North Atlantic Net CRF (in W/m^2). a) 5-year average of highest hurricane days but excluding all the time having detectable hurricanes b) 5 year average of lowest hurricane days but excluding all the time having detectable hurricanes c) the difference between a) and b).

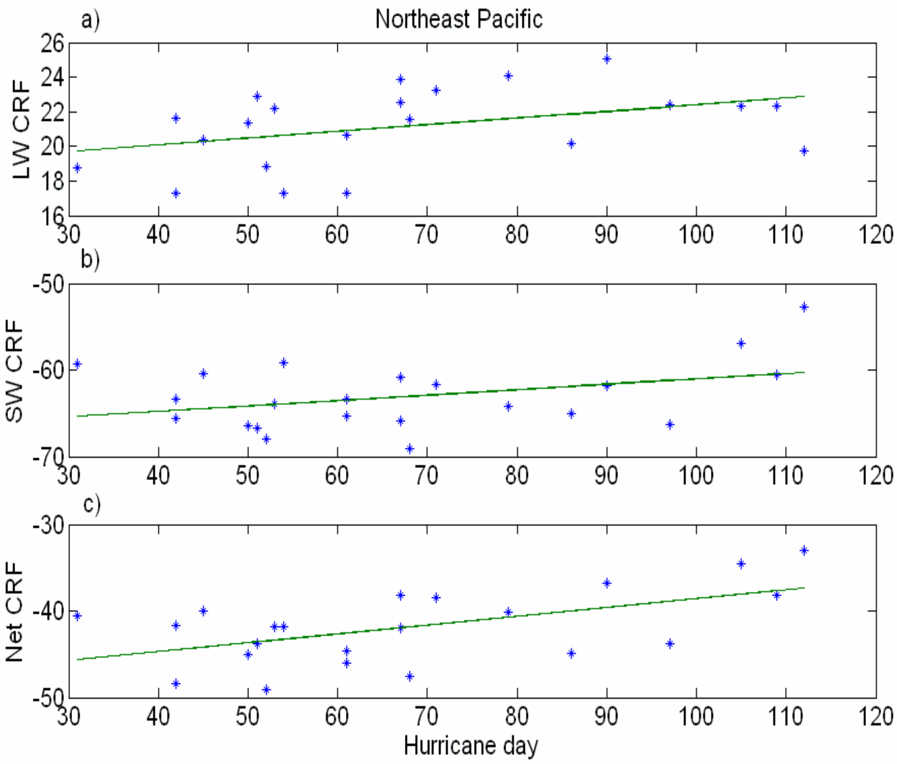

Fig. 16. Relationship of CRFs (in W/m^2) and hurricanes days for Northeast Pacific.

a) LW, S = 0.10 ± 0.07, R = 0.56

b) SW, S = 0.04 ± 0.04, R = 0.40

c) Net, S = 0.06 ± 0.07, R = 0.38

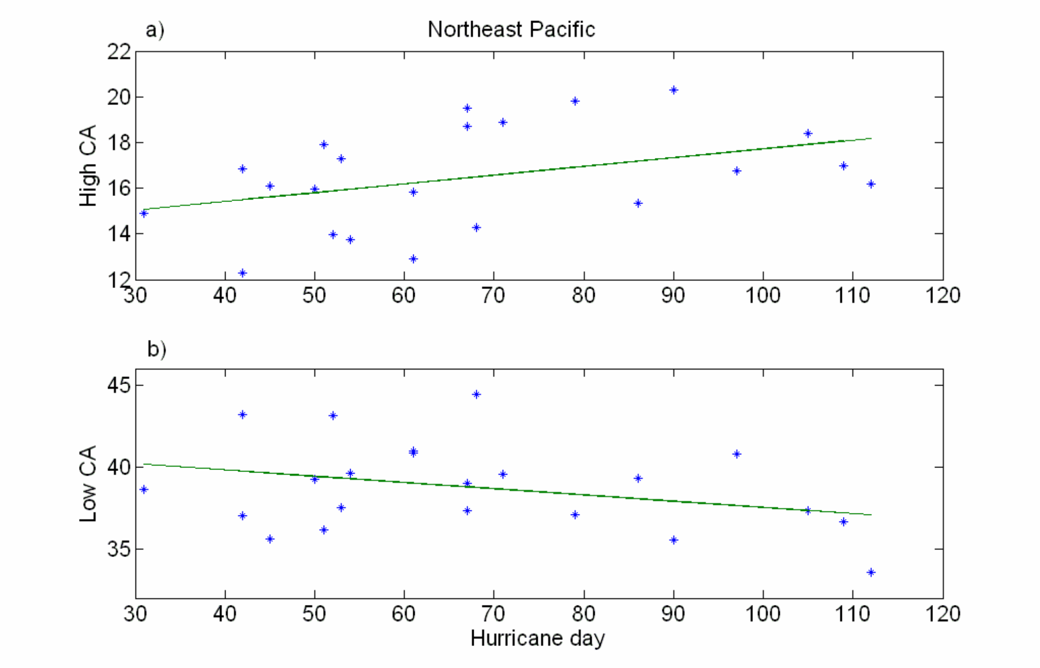

Fig. 17. Relationship of CA (in %) and hurricane days for Northeast Pacific.
a) High CA, S = 0.04 ± 0.04, R = 0.4
b) Low CA, S = –0.04 ± 0.05, R = –0.33

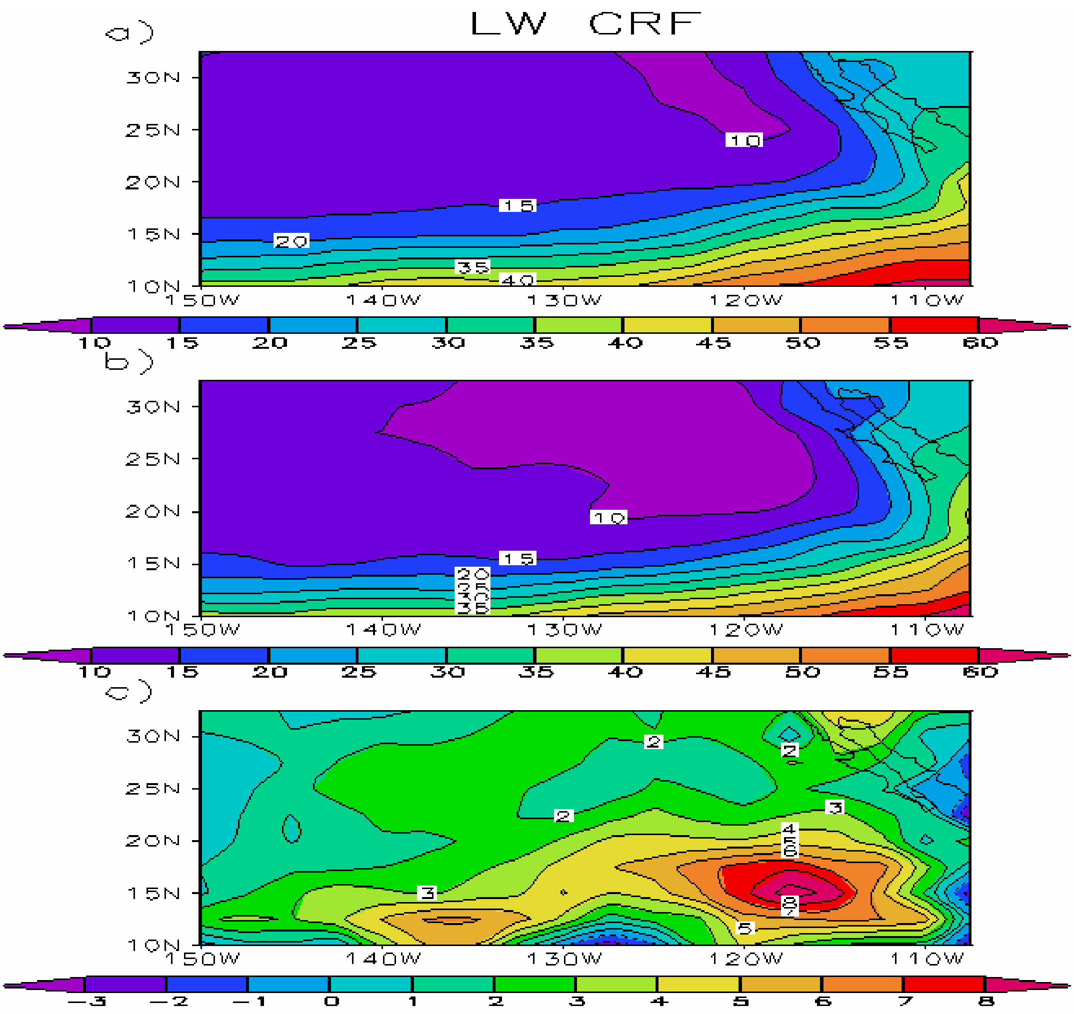

Fig. 18. Composite study of Northeast Pacific LW CRF (in W/m^2). a) 5-year average of highest hurricane days. b) 5-year average of lowest hurricane days. c) the difference between a) and b).

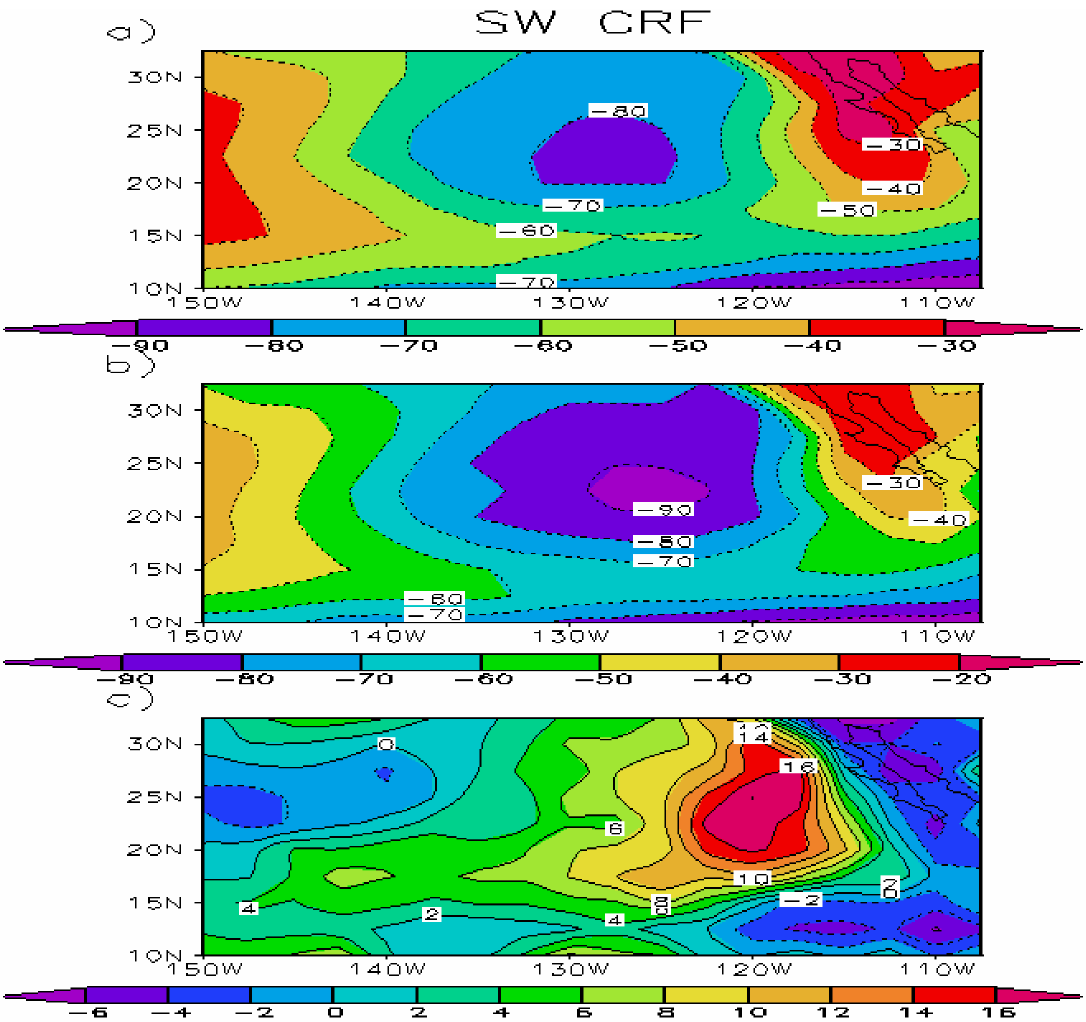

Fig. 19. Composite study of Northeast Pacific SW CRF (in W/m^2). a) 5-year average of highest hurricane days. b) 5-year average of lowest hurricane days. c) the difference between a) and b).

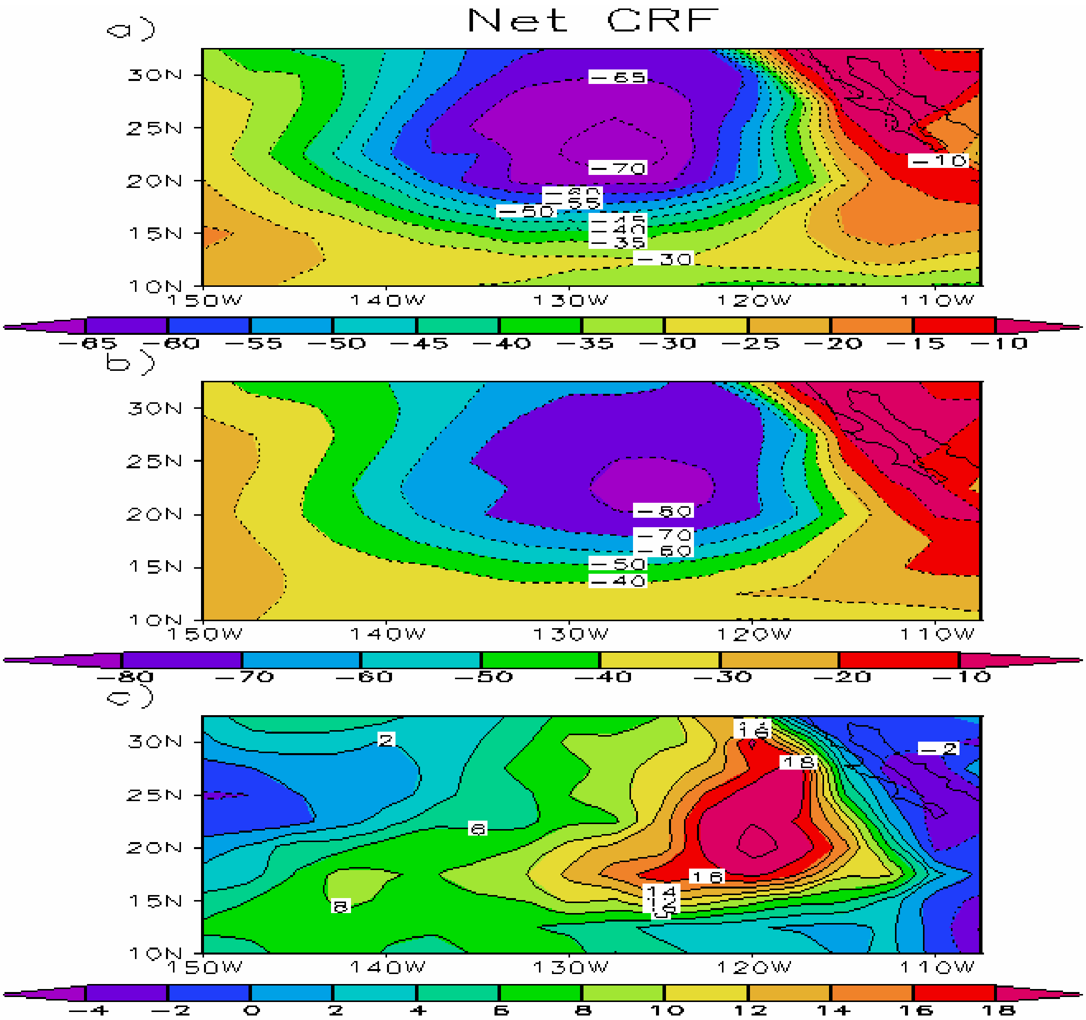

Fig. 20. Composite study of Northeast Pacific Net CRF (in W/m^2). a) 5-year average of highest hurricane days. b) 5-year average of lowest hurricane days. c) the difference between a) and b).

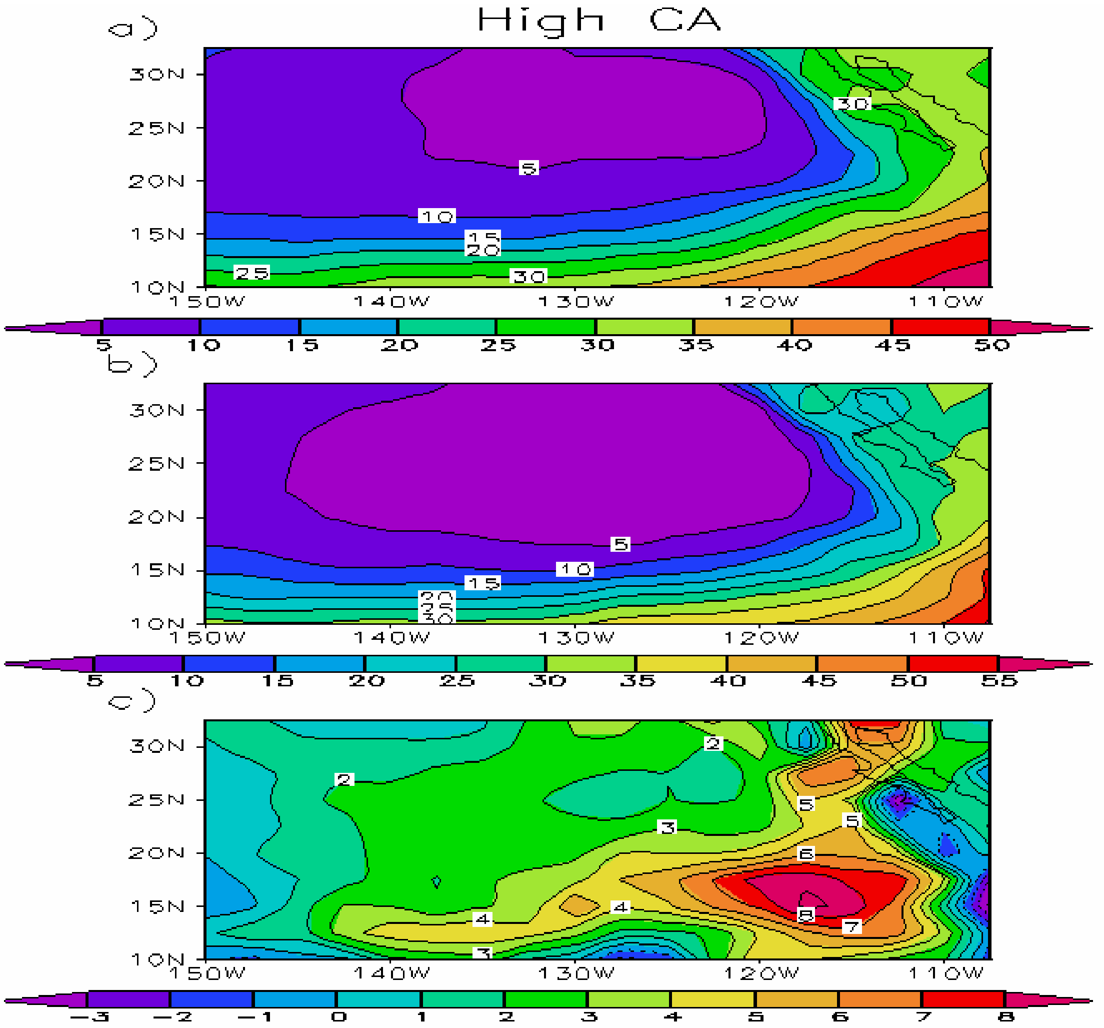

Fig. 21. Composite study of Northeast Pacific High CA (in %). a) 5-year average of highest hurricane days. b) 5-year average of lowest hurricane days. c) the difference between a) and b).

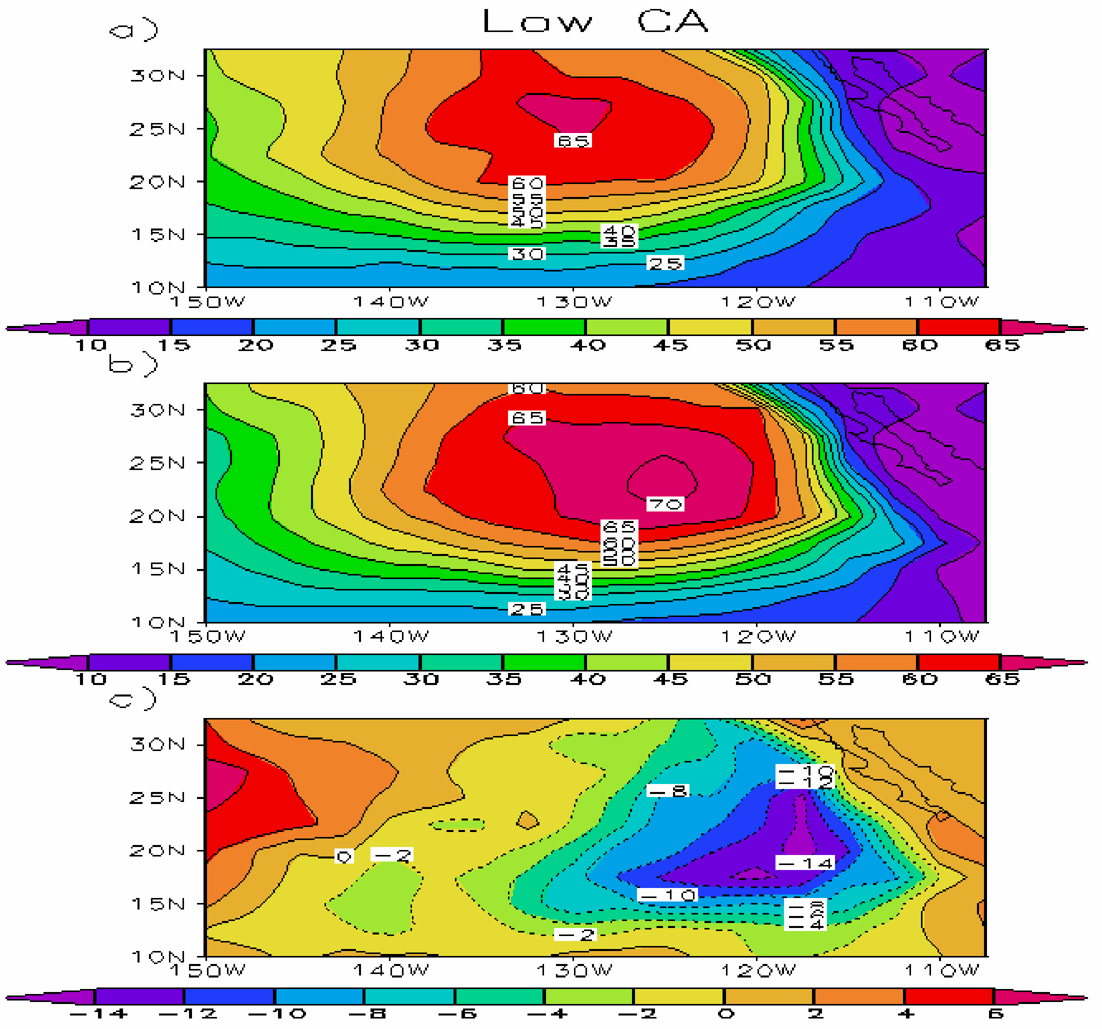

Fig. 22. Composite study of Northeast Pacific Low CA (in %). a) 5-year average of highest hurricane days. b) 5-year average of lowest hurricane days. c) the difference between a) and b).

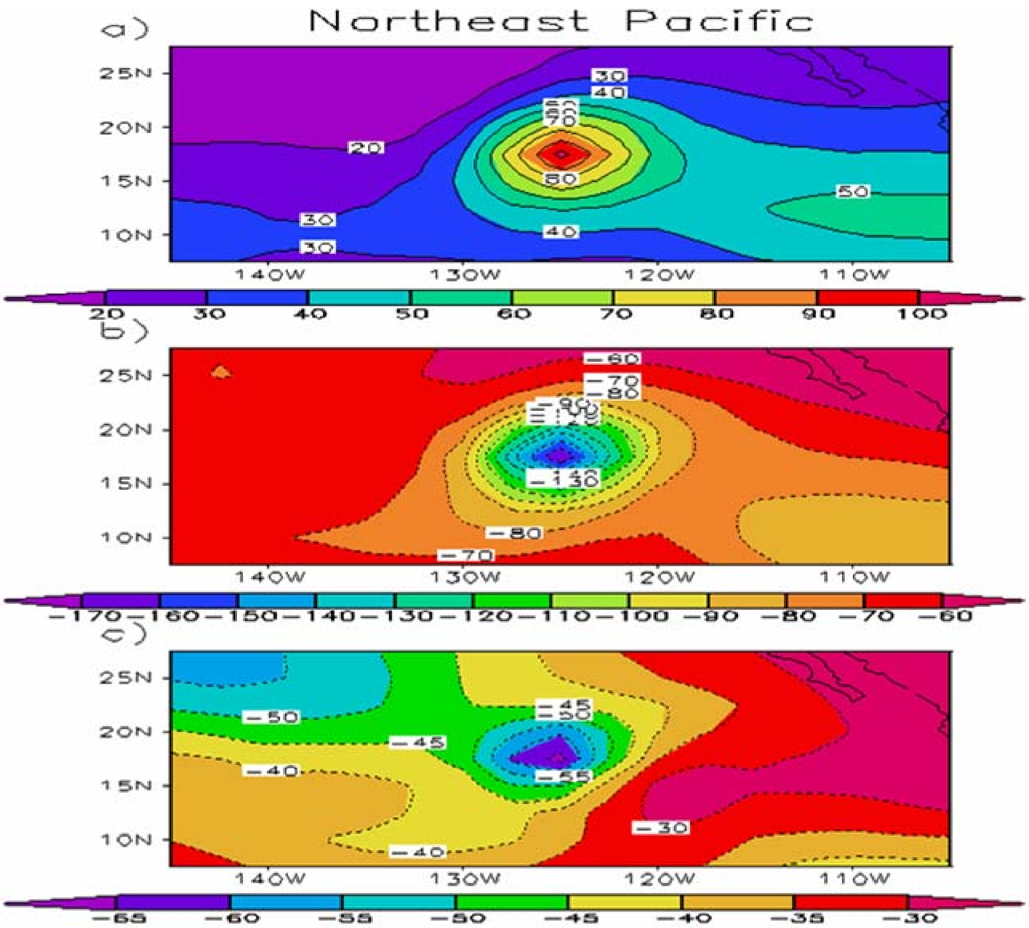

Fig. 23. Composite study of Northeast Pacific individual hurricanes CRFs (in W/m^2). All detectable hurricane center locations from 1983-2004, which are available every 6 hours, are taken as the center of a moving coordinate, and instantaneous CRFs are averaged relative to the coordinate center. Latitudinally 20 degrees on each side of hurricane center, and longitudinally 10 degrees on each side. The lat/long of hurricane center in the graph is the average of all available hurricane location for Northeast Pacific. a) LW b) SW c) Net.

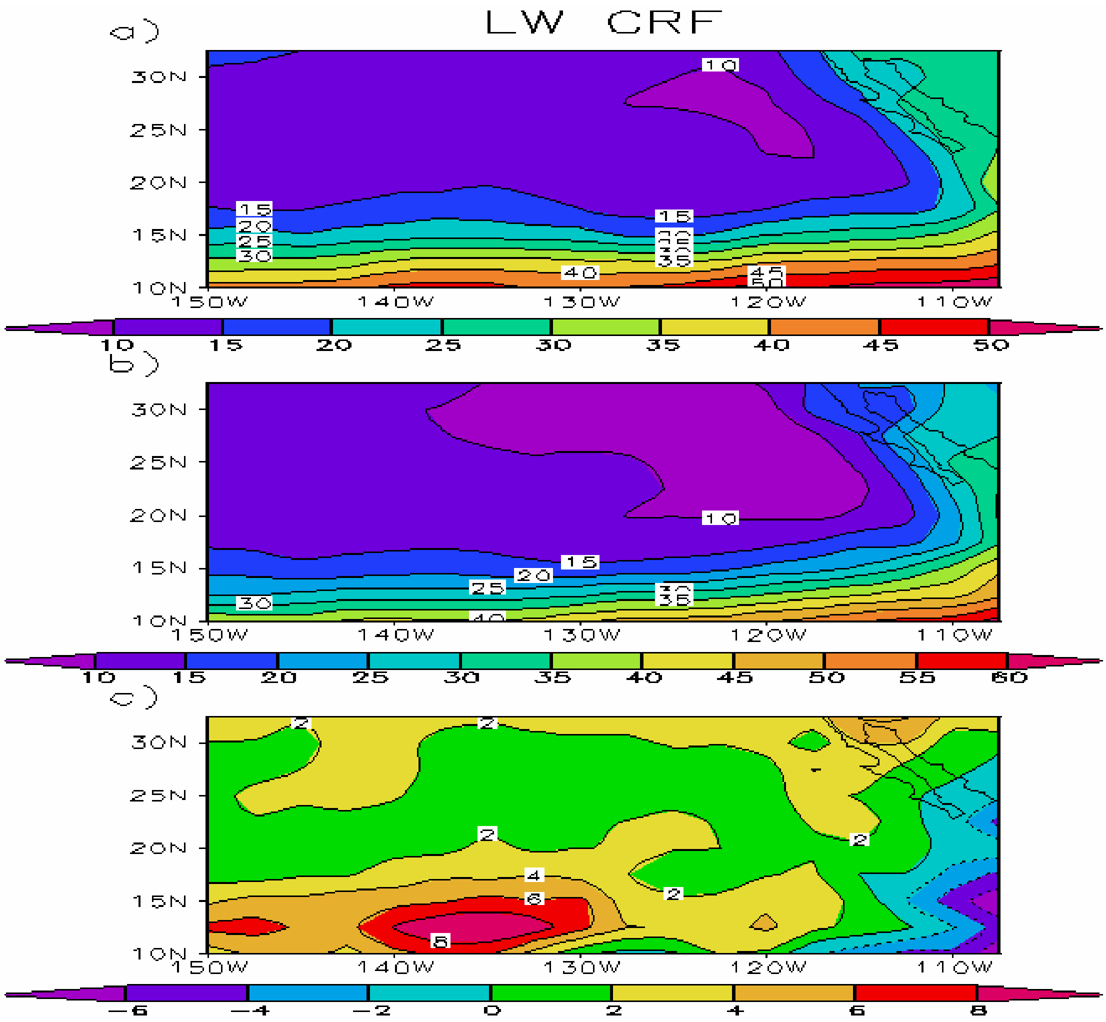

Fig. 24. Composite study of Northeast Pacific LW CRF (in W/m^2). a) 5-year average of highest hurricane days but excluding all the time having detectable hurricanes b) 5 year average of lowest hurricane days but excluding all the time having detectable hurricanes c) the difference between a) and b).

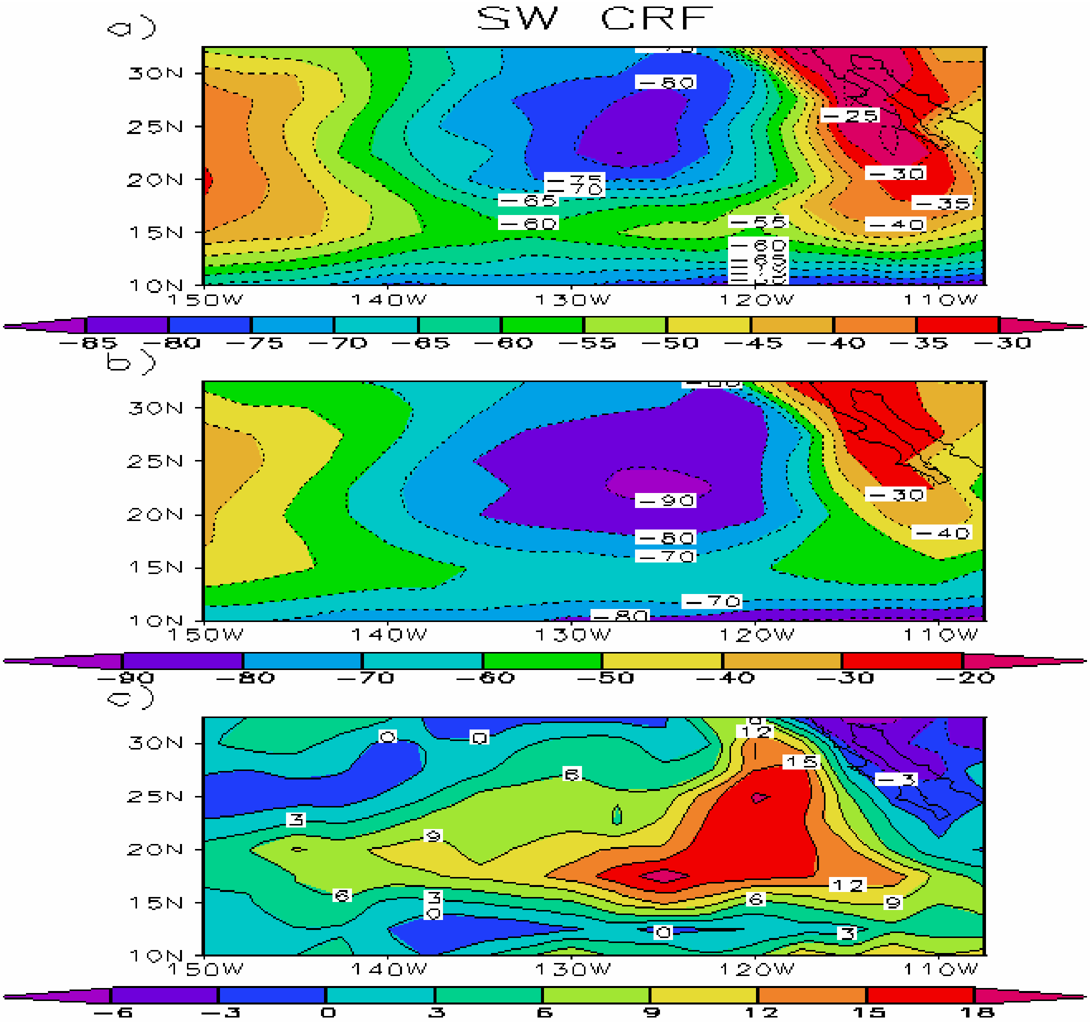

Fig. 25. Composite study of Northeast Pacific SW CRF (in W/m^2). a) 5-year average of highest hurricane days but excluding all the time having detectable hurricanes b) 5 year average of lowest hurricane days but excluding all the time having detectable hurricanes c) the difference between a) and b).

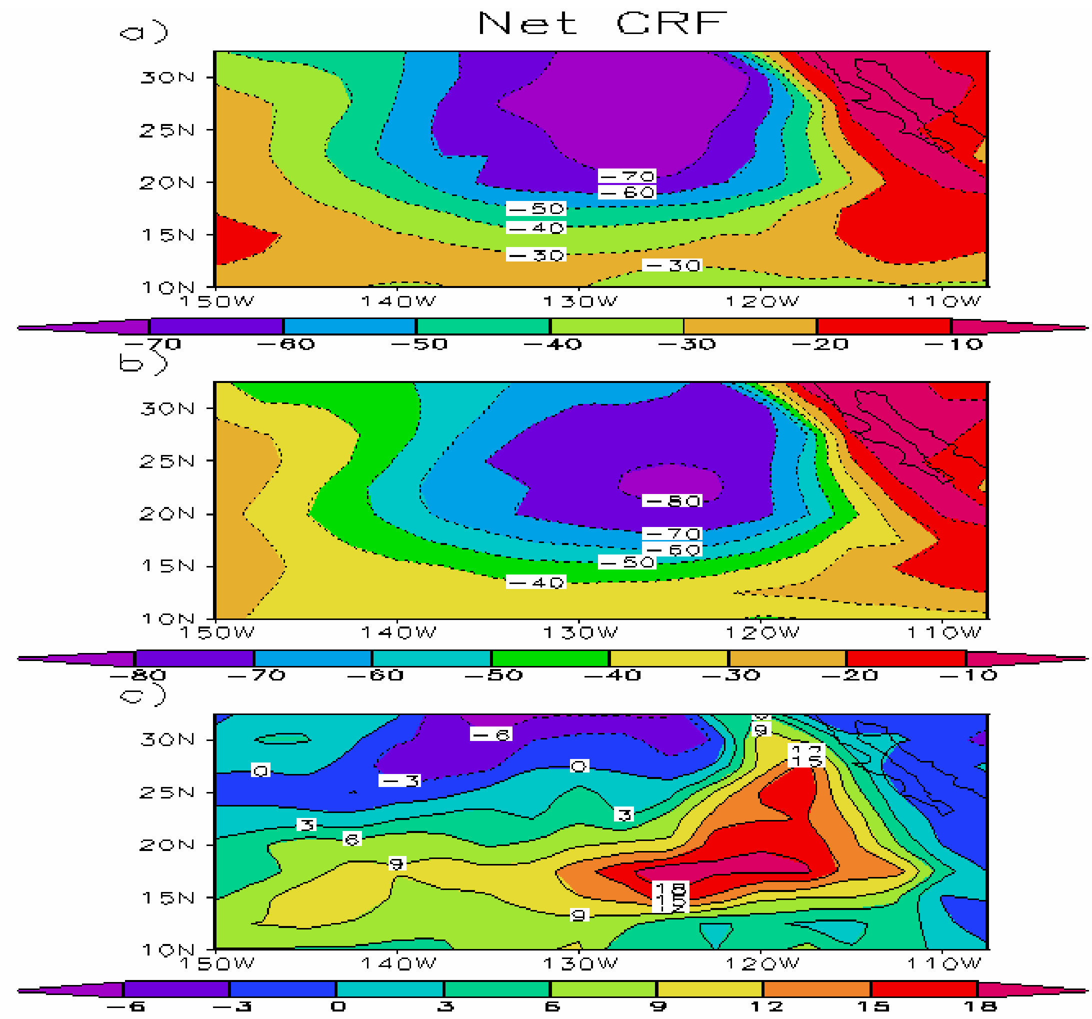

Fig. 26. Composite study of Northeast Pacific Net CRF (in W/m^2). a) 5-year average of highest hurricane days but excluding all the time having detectable hurricanes b) 5 year average of lowest hurricane days but excluding all the time having detectable hurricanes c) the difference between a) and b).

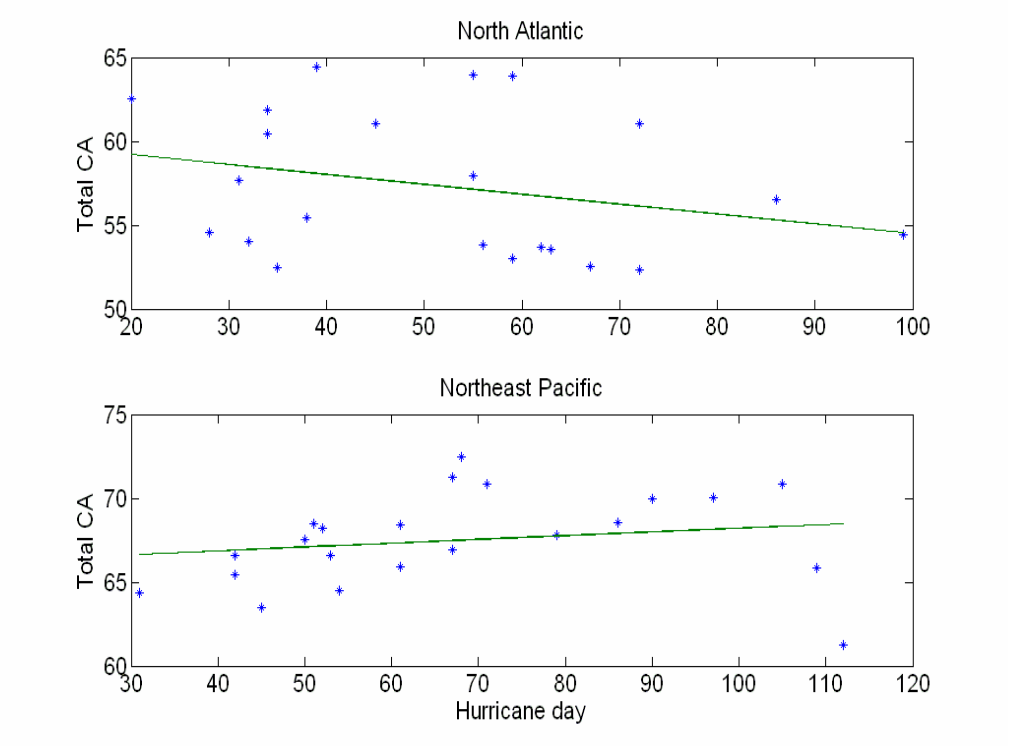

Fig. 27. Relationship of Total CA (in %) and hurricane days for
a) North Atlantic, S = 0.02 ± 0.05, R = 0.19
b) Northeast Pacific, S = –0.06 ± 0.10, R = –0.28